Superconductivity in the "Hot Spots" Model of the Pseudogap State: Impurity Scattering and Phase Diagram

N.A.Kuleeva*, E.Z.Kuchinskii†, M.V.Sadovskii‡
Institute for Electrophysics, Russian Academy of Sciences, Ekaterinburg, 620016, Russia

We analyze the anomalies of superconducting state (both s and d-wave pairing) in the model of the pseudogap state induced by Heisenberg spin fluctuations of antiferromagnetic short – range order, and based on the scenario of strong scattering near the "hot spots" on the Fermi surface. We present microscopic derivation of Ginzburg – Landau expansion, taking into account *all* Feynman graphs of perturbation theory for electron interaction with fluctuations of short – range order and in the "ladder" approximation for electron scattering by normal (nonmagnetic) impurities. We determine the dependence of superconducting critical temperature T_c and other characteristics of a superconductor on the parameters of the pseudogap and impurity scattering. It is shown that within this model it is possible to explain the typical phase diagram of high – temperature superconductors.

PACS numbers: PACS numbers: 74.20.Fg, 74.20.De

INTRODUCTION

One of the main problems in the physics of high – temperature superconducting cuprates remains the theoretical understanding of typical phase diagram of these compounds [1]. Especially interesting is the clarification of the nature of the pseudogap state which is observed in a wide region of temperatures and concentration of carriers [2], and is obviously crucial for the formation of electronic properties both in normal and superconducting states. Despite continuing discussions on the nature of the pseudogap, it seems that the preferable "scenario" of its formation is, in our opinion, based on the on the model of strong scattering of current carriers by antiferromagnetic (AFM, SDW) spin fluctuations of short – range order[1] [2, 3]. In momentum representation this scattering transfers momenta of the order of $\mathbf{Q} = (\frac{\pi}{a}, \frac{\pi}{a})$ (a – lattice constant of two – dimensional lattice) and leads to the "precursors" of spectrum transformation, taking place after the establishment of long – range AFM order (period doubling). As a result we obtain non – Fermi liquid like behavior (dielectrization) of spectral density in the vicinity of the so called "hot spots" on the Fermi surface, appearing at intersections of this surface with "would be" antiferromagnetic Brillouin zone boundary [2].

Within this approach a simplified model of the pseudogap state was actively studied [4, 5], under the assumption that the scattering by dynamic spin fluctuations can be reduced (which is valid for high enough temperatures) to a static Gaussian random field (quenched disorder) of pseudogap fluctuations with characteristic scattering vector from the vicinity of $\mathbf{Q}$, the width of which is determined by the inverse correlation length of short – range order $\kappa = \xi^{-1}$. The review of this approach with applications to the properties of the normal state and for some oversimplified models of pseudogap fluctuations influence on superconductivity can be found in Ref. [2].

In a recent paper [6] we have presented microscopic derivation of Ginzburg – Landau expansion[2] and studied the influence of pseudogap fluctuations in the model of "hot spots" on the main characteristics of superconducting state (both for s-wave and d-wave pairing), forming "on the background" of these fluctuations. In this paper we have considered slightly oversimplified version of our model, where Heisenberg – like spin fluctuations were replaced either by Ising – like, or by spin – independent charge (CDW) fluctuations. It was shown that such fluctuations of "dielectric" nature generally suppress superconductivity, leading to the drop of superconducting transition temperature and of specific heat discontinuity at the transition, as well as to a number of other anomalies. We also discovered two possible classes of superconducting order parameter interaction with pseudogap fluctuations, leading to significantly different scales of suppression of superconducting state.

The aim of the present paper is the generalization of the approach of Ref. [6] to the "realistic" case of Heisenberg spin fluctuations, as well as the account of (nonmagnetic) impurity (disorder) scattering influence on superconductivity

* E-mail: strigina@iep.uran.ru
† kuchinsk@iep.uran.ru
‡ E-mail: sadovski@iep.uran.ru
[1] Similar charge (CDW) fluctuations also cannot be excluded.
[2] Similar analysis based on Gorkov's equations was given in Ref. [7]

in the pseudogap state. It will be shown that this model allows for semiquantitative modeling of the typical phase diagram of a high – temperature superconductor.

"HOT SPOTS" MODEL AND RECURSION PROCEDURE FOR GREEN'S FUNCTION AND VERTICES.

Main results of our approach to the "hot spots" model and calculation of a single – particle Green's function in this model were described in detail in Refs. [4, 5], methods of calculation for the appropriate vertex parts were discussed in Refs. [6, 8]. Here we only present the main equations and definitions, giving a short description of changes necessary to take into account the spin structure of interaction in Heisenberg model of antiferromagnetic fluctuations.

Effective interaction of electrons with spin fluctuations in the model of "nearly antiferromagnetic" Fermi – liquid [4] is described by dynamic susceptibility, characterized by experimentally determined correlation length ξ and frequency ω_{sf} of spin fluctuations, which can depend both on concentration of carriers (and in case of ξ also on temperature), Both dynamic susceptibility and effective interaction are peaked (in momentum representation) in the vicinity of $\mathbf{Q} = (\pi/a, \pi/a)$, which leads to the appearance of two types of quasiparticles – "hot" one, with momenta close to the points on the Fermi surface, connected by scattering vectors $\sim \mathbf{Q}$, and "cold" one, with the momenta close to the parts of the Fermi surface, surrounding diagonals of the Brillouin zone [2, 4, 5].

For high enough temperatures $2\pi T \gg \omega_{sf}$ and we can neglect spin dynamics [4]. Electron interaction with spin (pseudogap) fluctuations reduces then to elastic scattering by appropriate static Gaussian random field. In this model it is possible to introduce a simplified form of effective interaction (correlator of this random field) [4, 5], which allows to perform full summation of the Feynman perturbation series, and obtain the following recursion procedure determining the single – electron Green's function:

$$G_k(\varepsilon_n \mathbf{p}) = \frac{1}{i\varepsilon_n - \xi_k(\mathbf{p}) + ikv_k\kappa - \Sigma_k(\varepsilon_n \mathbf{p})} \tag{1}$$

$$\Sigma_k(\varepsilon_n \mathbf{p}) = W^2 s(k+1) G_{k+1}(\varepsilon_n \mathbf{p}) \tag{2}$$

which is depicted as a symbolic "Dyson like" equation in Fig. 1 (a), where we have also introduced:

$$G_{0k}(\varepsilon_n \mathbf{p}) = \frac{1}{i\varepsilon_n - \xi_k(\mathbf{p}) + ikv_k\kappa} \tag{3}$$

Here $\kappa = \xi^{-1}$ is the inverse correlation length of pseudogap fluctuations, $\varepsilon_n = 2\pi T(n + 1/2)$ (for definiteness we assume here $\varepsilon_n > 0$),

$$\xi_k(\mathbf{p}) = \begin{cases} \xi_{\mathbf{p}+\mathbf{Q}} & \text{for odd } k \\ \xi_{\mathbf{p}} & \text{for even } k \end{cases} \tag{4}$$

$$v_k = \begin{cases} |v_x(\mathbf{p}+\mathbf{Q})| + |v_y(\mathbf{p}+\mathbf{Q})| & \text{for odd } k \\ |v_x(\mathbf{p})| + |v_y(\mathbf{p})| & \text{for even } k \end{cases} \tag{5}$$

where $\mathbf{v}(\mathbf{p}) = \frac{\partial \xi_{\mathbf{p}}}{\partial \mathbf{p}}$ is the velocity of a free quasiparticle with the spectrum $\xi_{\mathbf{p}}$, which is taken in a standard form [4]:

$$\xi_{\mathbf{p}} = -2t(\cos p_x a + \cos p_y a) - 4t' \cos p_x a \cos p_y a - \mu \tag{6}$$

where t is the transfer integral between nearest neighbors, and t' — between second nearest neighbors on the square lattice, a is the lattice constant, μ is the chemical potential.

Parameter W with dimension of energy defines the effective width of the pseudogap. In the model of Heisenberg spin fluctuations it can be written as [4]:

$$W^2 = g^2 \frac{< \mathbf{S}_i^2 >}{3} = g^2 < (n_{i\uparrow} - n_{i\downarrow})^2 > \tag{7}$$

where g is an interaction constant of electrons with spin fluctuations, $< \mathbf{S}_i^2 >$ is the average square of the spin on a lattice site, $n_{i\uparrow}$, $n_{i\downarrow}$ – operators of electron number at a site, with given spin directions. It is clear that similarly

to correlation length ξ, the value of W, in our semiphenomenological approach [4, 5], is also some function of carrier concentration (and temperature), to be determined from the experiment.

The value of $s(k)$ is determined by combinatorics of Feynman diagrams. For the simplest case of commensurate charged (CDW) pseudogap fluctuations :

$$s(k) = k \tag{8}$$

while for the most interesting case of Heisenberg spin (SDW) fluctuations [4][3]:

$$s(k) = \begin{cases} \frac{k+2}{3} & \text{for odd } k \\ \frac{k}{3} & \text{for even } k \end{cases} \tag{9}$$

Conditions of applicability of our approximations were discussed in detail in Refs. [4, 5].

Remarkable property of our model is the possibility of complete summation of all Feynman diagrams for the vertex parts[4], describing system response to an arbitrary external perturbation [8]. Here we just give appropriate recursion relations for "triangular" vertex in Cooper channel, similar to those derived in Ref. [6] in particle – particle channel, and describing the response to an arbitrary fluctuation of superconducting order parameter (gap):

$$\Delta(\mathbf{p}, \mathbf{q}) = \Delta_{\mathbf{q}} e(\mathbf{p}) \tag{10}$$

where the symmetry factor, corresponding to the type (symmetry) of the pairing, takes the following form:

$$e(\mathbf{p}) = \begin{cases} 1 & (\ s\text{-wave pairing}) \\ \cos p_x a - \cos p_y a & (\ d_{x^2-y^2}\text{-wave pairing}) \end{cases} . \tag{11}$$

and we always assume singlet pairing. The vertex of interest to us can be written as:

$$\Gamma(\varepsilon_n, -\varepsilon_n, \mathbf{p}, -\mathbf{p}+\mathbf{q}) \equiv \Gamma_{\mathbf{p}}(\varepsilon_n, -\varepsilon_n, \mathbf{q}) e(\mathbf{p}) \tag{12}$$

Then $\Gamma_{\mathbf{p}}(\varepsilon_n, -\varepsilon_n, \mathbf{q})$ is determined from recursion procedure of the following form:

$$\Gamma_{\mathbf{p}^k-1}(\varepsilon_n, -\varepsilon_n, \mathbf{q}) = 1 \pm W^2 r(k) G_k(\varepsilon_n, \mathbf{p}+\mathbf{q}) G_k(-\varepsilon_n, \mathbf{p}) \Bigg\{ 1 + \\ + \frac{2ik\kappa v_k}{G_k^{-1}(\varepsilon_n, \mathbf{p}+\mathbf{q}) - G_k^{-1}(-\varepsilon_n, \mathbf{p}) - 2ik\kappa v_k} \Bigg\} \Gamma_{\mathbf{p}^k}(\varepsilon_n, -\varepsilon_n, \mathbf{q}) \tag{13}$$

which is shown diagrammatically in Fig. 1 (b). "Physical" vertex is given by $\Gamma_{\mathbf{p}^k=0}(\varepsilon_n, -\varepsilon_n, \mathbf{q})$. Additional combinatorial factor $r(k) = s(k)$ for the simplest case of charged (or Ising – like spin) pseudogap fluctuations, analyzed in Ref. [6]. For the most interesting case of Heisenberg spin (SDW) fluctuations, analyzed below, this factor is givwn by [4] (Cf. also Appendix):

$$r(k) = \begin{cases} k & \text{for even } k \\ \frac{k+2}{9} & \text{for odd } k \end{cases} \tag{14}$$

The choice of the sign before W^2 in the r.h.s of Eq. (13) depends on the symmetry of superconducting order parameter and the type of pseudogap fluctuations [6] (see details in the Appendix). Different variants are given in Table I.

Table I. The choice of the sign in the recursion procedure for the vertex part.

Pairing	CDW - fluctuations	SDW - fluctuations (Ising)	SDW - fluctuations (Heisenberg)
s	+	−	+
d	−	+	−

It particular, from this Table we can see, that in the most interesting case of d-wave pairing and Heisenberg spin fluctuations, we must take this sign "−", so that alternating signs appear in our recursion procedure for the vertex part. However, for the case of s-wave pairing and the same type of pseudogap fluctuations, we must take "+", and there is no sign alternation in the recursion procedure. It Ref. [6] it was shown (for other cases shown in Table I), that this difference in the signs behavior of the recursion procedure for the vertex part leads to two cases of qualitatively different behavior of all the main characteristics of a superconductor.

---

[3] Detailed analysis of diagram combinatorics for Heisenberg model of spin fluctuations is given in the Appendix.

[4] Including all diagrams with intersecting interaction lines.

IMPURITY SCATTERING.

Scattering of electrons by normal (nonmagnetic) impurities can easily be taken into account in self – consistent Born approximation, writing down "Dyson" equation for the single – electron Green's function, shown graphically in Fig. 2 (a), where in addition to contribution shown in Fig. 1 (a), we have included the standard self – energy part due to impurity scattering [9]. As a result we obtain the recursion relation for the Green's function as:

$$G_k(\varepsilon_n \mathbf{p}) = \frac{1}{G_{0k}^{-1}(\varepsilon_n \mathbf{p}) - \rho U^2 \sum_{\mathbf{p}} G(\varepsilon_n \mathbf{p}) - W^2 s(k+1) G_{k+1}(\varepsilon_n \mathbf{p})} \tag{15}$$

where ρ is concentration of impurities with point – like potential U, and impurity contribution to self – energy contains fully dressed Green's function $G(\varepsilon_n \mathbf{p}) = G_{k=0}(\varepsilon_n \mathbf{p})$, to be determined self – consistently by our recursion procedure. As usual [9], contribution to this self – energy from real part of the Green's function is reduced to insignificant renormalization of the chemical potential, so that (15) can be written as:

$$G_k(\varepsilon_n \mathbf{p}) = \frac{1}{i(\varepsilon_n - \rho U^2 \sum_{\mathbf{p}} ImG(\varepsilon_n \mathbf{p}) + k v_k \kappa) - \xi_k(\mathbf{p}) - W^2 s(k+1) G_{k+1}(\varepsilon_n \mathbf{p})} \tag{16}$$

Thus, in comparison with impurity free case, we obtain, in fact, a simple substitution (renormalization):

$$\varepsilon_n \to \varepsilon_n - \rho U^2 \sum_{\mathbf{p}} ImG(\varepsilon_n \mathbf{p}) \equiv \varepsilon_n \eta_\epsilon \tag{17}$$

$$\eta_\epsilon = 1 - \frac{\rho U^2}{\varepsilon_n} \sum_{\mathbf{p}} ImG(\varepsilon_n \mathbf{p}) \tag{18}$$

If we do not perform fully self – consistent calculation of impurity self – energy, in the simplest approximation we just have:

$$\varepsilon_n \to \varepsilon_n - \rho U^2 \sum_{\mathbf{p}} ImG_{00}(\varepsilon_n \mathbf{p}) \equiv \varepsilon_n \eta_\epsilon = \varepsilon_n + \gamma_0 sign \varepsilon_n \tag{19}$$

$$\eta_\epsilon = 1 + \frac{\gamma_0}{|\varepsilon_n|} \tag{20}$$

where $\gamma_0 = \pi \rho U^2 N_0(0)$ is the standard Born impurity scattering rate [9] ($N_0(0)$ — density of states of free electrons on the Fermi level).

For "triangular" vertices of interest to us, the recurrence relation with the account of impurity scattering is shown graphically in Fig. 2 (b). For the vertex, describing interaction with the fluctuation of superconducting order parameter (10) with d-wave symmetry (11) this equation is significantly simplified, because the contribution of second diagram in the r.h.s. of Fig. 2 (b) is actually zero, because of validity of $\sum_{\mathbf{p}} e(\mathbf{p}) = 0$ (cf. discussion of similar situation in Ref. [10]). Then the recurrence equation for the vertex has the form of Eq. (13), where $G_k(\pm\varepsilon_n \mathbf{p})$ should be taken from Eqs. (15), (16), i.e. just replaced by dressed by impurity scattering, as defined in Fig. 2 (a). For the vertex describing interaction with fluctuations of the order parameter with s-wave symmetry, we have the following equation:

$$\Gamma_{\mathbf{p}k-1}(\varepsilon_n, -\varepsilon_n, \mathbf{q}) = 1 + \rho U^2 \sum_{\mathbf{p}} G(\varepsilon_n, \mathbf{p}+\mathbf{q}) G(-\varepsilon_n, \mathbf{p}) \Gamma_{\mathbf{p}}(\varepsilon, -\varepsilon_n, \mathbf{q}) \pm \tag{21}$$

$$\pm W^2 r(k) G_k(\varepsilon_n, \mathbf{p}+\mathbf{q}) G_k(-\varepsilon_n, \mathbf{p}) \left\{ 1 + \frac{2ik\kappa v_k}{G_k^{-1}(\varepsilon_n, \mathbf{p}+\mathbf{q}) - G_k^{-1}(-\varepsilon_n, \mathbf{p}) - 2ik\kappa v_k} \right\} \Gamma_{\mathbf{p}k}(\varepsilon_n, -\varepsilon_n, \mathbf{q})$$

where for $G_k(\pm\varepsilon_n \mathbf{p})$ we again use Eqs. (15), (16), and the sign before W^2 is determined in accordance with the rules formulated above. The difference with the case of the vertex for d-wave symmetry is the appearance of second term in the r.h.s. of Eq. (21), which reduces to the substitution:

$$1 \to \eta_\Gamma = 1 + \rho U^2 \sum_{\mathbf{p}} G(\varepsilon_n, \mathbf{p}+\mathbf{q}) G(-\varepsilon_n, \mathbf{p}) \Gamma_{\mathbf{p}}(\varepsilon, -\varepsilon_n, \mathbf{q}) \tag{22}$$

Thus our self– consistency procedure can be formulated in this case as follows: start from the "zeroth order" approximation $G = G_{00}$, $\Gamma_{\mathbf{p}} = 1$, i.e. simply take in Eqs.(16), (21) $\eta_\varepsilon = \eta_\Gamma = 1 - \rho U^2 / \varepsilon_n \sum_{\mathbf{p}} ImG_{00}(\varepsilon_n \mathbf{p})$. Perform

all necessary recursions (starting from some big enough value of k) and determine new values for $G = G_{k=0}$ and $\Gamma_{\mathbf{p}} = \Gamma_{k=0}$. Calculate again η_ε and η_Γ using (18) and (22), use these values in Eqs. (16), (21) etc., until convergence.

Analyzing the vertex with d-wave symmetry we just take $\eta_\Gamma = 1$ at all stages of calculation. In fact, in this case there is no need for achieving full self – consistency over impurity scattering, as it leads only to some small corrections to the results of non self – consistent calculation using the simplest substitution (19) [7].

SUPERCONDUCTING TRANSITION TEMPERATURE AND GIZBURG – LANDAU COEFFICIENTS.

Critical temperature of superconducting transition is determined from the equation for Cooper instability of the normal phase:

$$1 - V\chi(0;T) = 0 \tag{23}$$

where the generalized Cooper susceptibility is defined by diagram shown in Fig. 3 and is given by:

$$\chi(\mathbf{q};T) = -T\sum_{\varepsilon_n}\sum_{\mathbf{p}} G(\varepsilon_n\mathbf{p}+\mathbf{q})G(-\varepsilon_n,-\mathbf{p})e^2(\mathbf{p})\Gamma_{\mathbf{p}}(\varepsilon_n,-\varepsilon_n,\mathbf{q}) \tag{24}$$

Pairing constant V is assumed to be non zero in a layer of the width of $2\omega_c$ around the Fermi level, and determines the "bare" transition temperature T_{c0} in the absence of pseudogap fluctuations from the standard BCS equation[5]:

$$1 = \frac{2VT}{\pi^2}\sum_{n=0}^{\bar{m}}\int_0^{\pi/a} dp_x \int_0^{\pi/a} dp_y \frac{e^2(\mathbf{p})}{\xi^2_{\mathbf{p}} + \varepsilon^2_n} \tag{25}$$

where $\bar{m} = [\frac{\omega_c}{2\pi T_{c0}}]$ is dimensionless cutoff in the sum over Matsubara frequencies. Similar to Ref. [6] all calculations were performed for a typical spectrum of bare quasiparticles (6) for different relations between t, t' and μ. E.g. taking rather arbitrarily $\omega_c = 0.4t$ and $T_{c0} = 0.01t$ it is rather easy to find the value of pairing constant V in (25), responsible for this given value of T_{c0} for different types of pairing. For example, in the case of s-wave pairing we obtain $\frac{V}{ta^2} = 1$, while for the case of $d_{x^2-y^2}$-wave pairing we get $\frac{V}{ta^2} = 0.55$.

To calculate T_c we need only to know the Cooper susceptibility at $q = 0$, and this simplifies calculations considerably [6]. In general case, e.g. to calculate Ginzburg – Landau coefficients we need $\chi(q;T)$ at arbitrary (small) q.

Ginzburg – Landau expansion for the difference of free – energies of superconducting and normal states, written in a standard form:

$$F_s - F_n = A|\Delta_{\mathbf{q}}|^2 + q^2C|\Delta_{\mathbf{q}}|^2 + \frac{B}{2}|\Delta_{\mathbf{q}}|^4 \tag{26}$$

is determined from the usual loop expansion for the free – energy of electrons, moving in a random field of order parameter fluctuations (10).

It is convenient to normalize GL – coefficients A, B, C by their values in the absence of pseudogap fluctuations [6]:

$$A = A_0K_A; \qquad C = C_0K_C; \qquad B = B_0K_B, \tag{27}$$

where

$$A_0 = N_0(0)\frac{T-T_c}{T_c} < e^2(\mathbf{p}) >; \quad C_0 = N_0(0)\frac{7\zeta(3)}{32\pi^2T_c^2} < |\mathbf{v}(\mathbf{p})|^2e^2(\mathbf{p}) >;$$
$$B_0 = N_0(0)\frac{7\zeta(3)}{8\pi^2T_c^2} < e^4(\mathbf{p}) >, \tag{28}$$

and angular brackets denote usual averaging over the Fermi surface: $< \ldots >= \frac{1}{N_0(0)}\sum_p \delta(\xi_{\mathbf{p}})\ldots$, $N_0(0)$ is again the density of state on the Fermi level for free electrons.

---

[5] We do not discuss the physical nature of this interaction — it may be due to exchange by spin fluctuations, phonons, or by some combination of electron phonon and spin fluctuation mechanism.

Then we have the following general expressions [6]:

$$K_A = \frac{\chi(0;T) - \chi(0;T_c)}{A_0} \tag{29}$$

$$K_C = \lim_{q\to 0} \frac{\chi(\mathbf{q};T_c) - \chi(0;T_c)}{q^2 C_0} \tag{30}$$

$$K_B = \frac{T_c}{B_0} \sum_{\varepsilon_n} \sum_{\mathbf{p}} e^4(\mathbf{p}) (G(\varepsilon_n \mathbf{p}) G(-\varepsilon_n, -\mathbf{p}))^2 (\Gamma_{\mathbf{p}}(\varepsilon_n, -\varepsilon_n, 0))^4 \tag{31}$$

which were used for direct numerical computations.

In the presence of impurities all Green's functions and vertices entering these expressions are to be calculated using Eqs. (16) and (21).

The knowledge of GL – coefficients allows to determine all major characteristics of a superconductor close to the transition temperature T_c. E.g. the coherence length is defined as:

$$\frac{\xi^2(T)}{\xi^2_{BCS}(T)} = \frac{K_C}{K_A}, \tag{32}$$

where $\xi_{BCS}(T)$ is the value of coherence length in the absence of pseudogap.

Penetration depth is given by:

$$\frac{\lambda(T)}{\lambda_{BCS}(T)} = \left(\frac{K_B}{K_A K_C} \right)^{1/2}, \tag{33}$$

where we again normalized on the value of $\lambda_{BCS}(T)$ in the absence of pseudogap fluctuations.

The slope of the upper critical magnetic field close to T_c, normalized in a similar way, is given by:

$$\frac{\left|\frac{dH_{c2}}{dT}\right|_{T_c}}{\left|\frac{dH_{c2}}{dT}\right|_{T_{c0}}} = \frac{T_c}{T_{c0}} \frac{K_A}{K_C}. \tag{34}$$

Relative discontinuity of specific heat at the transition is defined as:

$$\Delta C = \frac{(C_s - C_n)_{T_c}}{(C_s - C_n)_{T_{c0}}} = \frac{T_c}{T_{c0}} \frac{K_A^2}{K_B}. \tag{35}$$

NUMERICAL RESULTS.

Numerical results for the case of charge (CDW) Ising – like spin (SDW) fluctuations of short – range (pseudogap) order were given in Ref. [6]. Here we shall concentrate on the analysis of most important and interesting case of Heisenberg spin (SDW) fluctuations and the role of impurity scattering (disorder). Due to importance of d-wave pairing for copper oxide superconductors, this case is analyzed in more details.

All calculations (in this section) were performed for typical values of parameters of the "bare" spectrum $t'/t = -0.4$, $\mu/t = -1.3$, while for the inverse correlation length we assumed $\kappa a = 0.2$. To spare space we do not present here explicit results for dimensionless GL – coefficients K_A, K_B, K_C, giving only the final results for the main physical characteristics of a superconductor.

For dependences on the effective width of the pseudogap we always present these characteristics normalized by the appropriate values at $T = T_{c0}$, while for the dependences on impurity scattering rate γ_0 we use normalization by appropriate values at $T = T_{c0}(W)$, i.e. at the "bare" critical temperature for a given value of W, but in the absence of impurities ($\gamma_0 = 0$).

d – wave pairing.

In Fig. 4 we show the dependence of superconducting transition temperature T_c on the effective pseudogap width W for several values of impurity scattering rate. It can be seen that pseudogap fluctuations lead to significant suppression of superconductivity and for finite disorder we always obtain some "critical" value of W, when T_c becomes zero. This suppression of T_c is naturally due to partial "dielectrization" of electronic spectrum in the vicinity of "hot spots" [4, 5].

Similar dependences for coherence length and penetration depth are shown in Fig. 5, those for the slope of the upper critical field and specific heat discontinuity at the transition — in Fig. 6. Typically we also observe fast suppression of these characteristics by pseudogap fluctuations.

Dependences on the value of correlation length of short – range order fluctuations is, generally, more smooth — in all cases the growth of ξ (drop of κ) enlarges the effects of pseudogap fluctuations. We do not show appropriate results to spare space.

In Fig. 7 we show dependences of superconducting transition temperature T_c on impurity scattering rate γ_0 for several values of the effective pseudogap width. It is seen that in the presence of pseudogap fluctuations T_c suppression with the growth of disorder is faster than in the absence of the pseudogap ($W = 0$), when the dependence of T_c on γ_0 in case of d-wave pairing, described by the standard Abrikosov – Gorkov curve [10, 11]. Analogous dependences for coherence length and penetration depth are shown in Fig. 8, while for the slope of the upper critical field $H_{c2}(T)$ and specific heat discontinuity — in Fig. 9. Again we see, that impurity scattering (disorder) leads to fast suppression of the last two characteristics, e.g. the effect of pseudogap fluctuations is enhanced by impurity scattering.

Dependences on parameters of the pseudogap, obtained above, are qualitatively similar to those found in Ref. [6] for the case of charged (CDW) pseudogap fluctuations, when we also are dealing with recursion procedure for the vertex part with alternating signs. At the same time certain differences appear here due another combinatorics of diagrams. Dependences on the impurity scattering rate (disorder) in this model were not studied previously[6].

These dependences are in qualitative agreement with majority of the data, obtained in experiments on copper oxide superconductors in the pseudogap region of the phase diagram (from underdoped to optimally doped region). Below we shall demonstrate that these results may be used for direct modeling of the typical phase diagram of these compounds.

s – wave pairing.

Analysis of the case of s-wave pairing is interesting mainly as demonstration of characteristic differences with the case of d-wave pairing. At present, there are no definite experimental data on s-wave superconductivity in systems with pseudogap, though it is quite possible that such systems will be discovered in some future.

Our calculations show that pseudogap fluctuations significantly suppress superconductivity also in this case (Fig. 10), though the characteristic scale of these fluctuations, necessary for a major suppression of the superconducting state, is much larger here than in the case of d-wave pairing. This result was obtained earlier in Ref. [6], though it is necessary to note that in the case of Heisenberg (SDW) fluctuations, considered here, there is no characteristic "plateau" in the dependence of T_c on W, which was obtained for the case of charged (CDW) pseudogap fluctuations in Ref. [6]. On the same scale of W takes place also the major suppression of specific heat discontinuity at superconducting transition, as shown at the insert in Fig. 10. Similar dependences for the coherence length and penetration depth are analogous to those obtained in Ref. [6] and we do not show these here. In Fig.11 we show dependences of T_c on impurity scattering (disorder). Besides relatively weak suppression of T_c by disorder, connected [7] with small suppression of the density of states at the Fermi level by disorder, we can observe also a weak growth of T_c with γ_0, which is apparently due some "smearing" of the pseudogap in the density of states.

In Fig. 12 we show impurity effects for the case of s-wave pairing on the coherence length and penetration depth.

Finally, in Fig. 13 we demonstrate the influence of impurity scattering (disorder) on the slope of the upper critical field and specific heat discontinuity. Again the specific heat discontinuity is significantly suppressed by disorder, while the slope of $H_{c2}(T)$ demonstrates qualitatively different behavior, than in the case of the d-wave pairing: the growth of disorder leads to the growth of this slope, as in the standard theory of "dirty" superconductors [20], while pseudogap

---

[6] Analysis of impurity dependence of T_c in Ref. [7] was performed for the case of recursion procedure without sign alternation, appearing for the case of Ising – like SDW fluctuations, when superconductivity suppression is much slower.

fluctuations further increase the slope of $H_{c2}(T)$. In the absence of pseudogap fluctuations, similar differences (between s-wave and d-wave cases) in the behavior of the slope of $H_{c2}(T)$ under disordering were noted earlier in Ref. [10].

MODELING OF THE PHASE DIAGRAM.

The described above model of the influence of pseudogap fluctuations on superconductivity allows to perform simple modeling of a typical phase diagram of high – temperature superconducting cuprates[7]. First attempt of such modeling in an oversimplified version of our model was made in Ref. [12]. The main idea is in identifying our parameter W with an experimentally observable effective width of the pseudogap (crossover temperature into pseudogap region of the phase diagram) $E_g \approx T^*$, which is determined by numerous experiments [1, 2, 3]. It is well known that this crossover temperature is practically linear in concentration of doping impurity (carrier concentration), starting at small concentration from the values of the order of 10^3K and going to zero at some critical concentration $x_c \approx 0.19..0.22$, which is slightly higher than the "optimal" value $x_o \approx 0.15..0.17$ [1, 13]. Accordingly, we can assume similar concentration dependence of our pseudogap parameter $W(x)$[8]. In this sense we can say that concentration dependence $W(x)$ directly follows from the experiment. Then the only parameter of the model to be determined remains the concentration dependence of the "bare" superconducting transition temperature $T_{c0}(x)$, which would have existed in the absence of pseudogap fluctuations. The knowledge of this dependence allows then to calculate the observed concentration dependence of superconducting transition temperature $T_c(x)$ solving equations of our model. Unfortunately, as was already noted in Ref. [6], concentration dependence $T_{c0}(x)$ is, in general case, unknown and is not determined from any known experiment. Thus, it remains the fitting parameter of our theory.

Assuming following Ref. [12] that $T_{c0}(x)$ can also be described by a linear function of concentration x, going to zero at $x = 0.3$, and varying the value of $T_{c0}(x = 0)$ to obtain the correct value of $T_c(x = x_o)$ it is possible to calculate the "observed" dependence of $T_c(x)$. An example of such calculation for the case of d-wave pairing and scattering by charged (CDW) pseudogap fluctuations [6], using typical dependence of $W(x)$, is shown in Fig. 14. It can be seen that even with such crude and rather arbitrary assumptions, the "hot spots" model allows to obtain the $T_c(x)$ dependence, which is pretty close to the experimentally observed. Similar calculations for the case of Ising – like model of interaction of electrons with spin fluctuations (no sign alternation in the recursion procedure for the vertex [6]) show that the reasonable values of $T_c(x)$ can only be obtained for rather unrealistic values of $W(x)$ about an order of magnitude higher than those observed experimentally.

Within our BCS – like model for the "bare" T_{c0}, an assumption of significant concentration dependence of this parameter seems rather unrealistic[9]. Thus, let us assume that the value of T_{c0} has no dependence on carrier (doping impurity) concentration x at all, but take into account the fact that introduction of doping impurity immediately leads to the appearance of some random impurity scattering of carriers (due to internal disorder), which can be simply described by introduction of some linearly growing impurity scattering rate $\gamma(x)$. Now let us just assume that this growth of internal disorder leads to complete suppression of d-wave pairing at $x = 0.3$, in accordance with Abrikosov – Gorkov dependence [10, 11]. Results of calculations for the phase diagram of $La_{2-x}Sr_xCuO_4$ – type system within this model, and for the case of Heisenberg pseudogap fluctuations and the described role of impurity scattering is shown in Fig. 15. The values of different parameters used in this calculation are shown at the same figure. "Experimental" values of $T_c(x)$, shown in this figure (as well as in Fig. 14) by "diamonds", were obtained from the empirical relation [13, 14]:

$$\frac{T_c(x)}{T_c(x = x_o)} = 1 - 82.6(x - x_o)^2 \tag{36}$$

which represents rather good fit to experimental data for concentration dependence of T_c in a number of cuprates. We can see that in all underdoped region our model gives practically ideal description of "experimental" data for quite reasonable values of $W(x)$. At the end of overdoped region agreement is less satisfactory, but it should be noted that both the relation (36) is not quite good here, and our model of superconductivity suppression in overdoped region

---

[7] We "neglect" here the existence of a narrow region of antiferromagnetic ordering in Mott dielectric appearing at low concentrations of doping impurity, limiting our analysis to a wide region of a "bad" metal.

[8] Obviously, this identification can be done up to some unknown factor ~ 1.

[9] Within this approach any dependence of T_{c0} on x can only be due to some weak concentration dependence of the density of states on the Fermi level.

is obviously too crude. Also it should be noted that we have not performed any special fitting of parameters of our model to increase agreement in this region.

It is interesting to analyze the behavior of superconducting transition temperature T_c under additional disordering at different compositions (concentrations of carriers). There were numerous experimental studies with such disordering being introduced by additional impurities [16, 17] or by irradiation by fast neutrons [15] and electrons [18, 19]. Special discussion of the role of such additional disordering in the context of the existence of the pseudogap state was presented, apparently, only in Ref. [17].

In our model such additional disordering is easily simulated by the introduction of an additional impurity scattering rate γ_0, which is just added to our parameter of an internal disorder $\gamma(x)$. Results of our calculations for two values of this parameter are also shown in Fig. 15. We can see, that in complete agreement with experiments [17], introduction of additional "impurities" (disorder) leads to rather fast reduction of the superconductivity region on the phase diagram Also in complete agreement with our conclusion made above with respect to Fig. 7 and with the results of experiments [15, 17], superconductivity suppression by disordering in underdoped (pseudogap) region is significantly faster, than for optimal doping. It could be expected that introduction of "normal" disorder, obviously leading to some suppression of the pseudogap in the density of states, could have lead to some "slowing down" of T_c suppression. However, our calculations show that such effect in the case of d-wave pairing is just absent.

The problem, however, is that in all cases our calculations show that T_c suppression is faster than it is predicted by the standard Abrikosov – Gorkov curve in case of d-wave pairing [10, 11]. At the same time, most attempts to fit experimental data on disordering in cuprates [16, 18, 19], show that such suppression is in fact significantly *slower*, than predicted by Abrikosov – Gorkov dependence. This fact remains one of the major unsolved problems of the theory of high – temperature superconductors [20]. One of the possible solutions of this problem may be connected with rigorous description of disordering effects in superconductors, which belong to transition region from "large" pairs of BCS theory to "compact" pairs (bosons), appearing in the limit of very strong coupling [21]. Another interesting possibility to explain the "slowing down" of T_c suppression is connected with an account of anisotropy of impurity scattering, analyzed in detail in Refs. [10, 22]. This effect can be rather easily included in our calculational scheme. It seems especially significant in connection with the established strong anisotropy of elastic scattering (with d-wave symmetry), observed in ARPES experiments on $Bi_2Sr_2CaCu_2O_{8+\delta}$ [23, 24]. Appropriate scattering rate changes in the interval of $20 - 60meV$ [24], which is nearly an order of magnitude higher, than the maximal value of $\gamma(x)$, used in our calculations, which once again demonstrates an unusual stability of d-wave pairing in cuprates towards static disorder. It should be noted that our model of electron self – energy in fact describes analogous anisotropy of elastic scattering, corresponding to its growth in the vicinity of "hot spots", but we do not observe the effect of the "slowing down" of T_c suppression in our calculations.

Our results show that despite the obvious crudeness of our assumptions, the "hot spots" model allows to obtain rather reasonable (even semiquatitative) description of the region of existence of superconducting state on the phase diagram of high – temperature superconducting cuprates[10]. The main deficiency of our approach remains rather indeterminate scenario for concentration dependence of the "bare" superconducting transition temperature.

CONCLUSION

The analysis presented above shows, that the model of the pseudogap state, based on the concept of "hot spots", can provide a reasonable description of the main properties of the superconducting phase of cuprates, as well as of the phase diagram, using relatively small number of fitting parameters, most of which can be determined from independent experiments.

Let us stress that all calculations were performed using the standard assumption of self – averaging nature of superconducting order parameter (gap) over the random fields of impurities and pseudogap fluctuations. Usually this assumption is justified for superconductors with coherence lengths (size of Cooper pairs) much exceeding the other microscopic lengths in the system, such as mean free path or correlation length of pseudogap fluctuations ξ.

In the class of models of the pseudogap state under consideration this assumption is not, in general, valid and important effects due to non self – averaging [25, 26], which lead to a qualitatively new picture of inhomogeneous superconducting state, with "drops" of superconducting phase existing for temperatures $T > T_c$. In principle, there are

---

[10] Above we always assumed that we are dealing with hole – doped cuprates, where concentration dependence of $T^*(x)$ is well established [1, 13]. For electron doped systems the data on the pseudogap state are rather fragmentary.

experimental data, directly supporting such picture of inhomogeneous superconductivity in cuprates [27, 28, 29]. Of course, we are far from claiming, that these experiments directly support oversimplified theoretical models developed in Refs. [25, 26]. At the same time, these results stress the importance of rigorous analysis of non self – averaging effects in relatively "realistic" models of the pseudogap state, such as the "hot spots" model, described above[11].

This work was supported in part by the RFBR grant No. 02-02-16031, as well as by the program of fundamental research "Quantum macrophysics" of the Presidium of RAS, the program "Strongly correlated electrons in semiconductors, metals, superconductors and magnetic materials" of the RAS Department of Physical Sciences, and also under the project of the Ministry of Education and Science of the Russian Federation "Studies of collective and quantum effects in condensed matter".

[11] The picture of "superconducting drops", existing above T_c allows to understand a number of experiments, which are usually interpreted as supporting the superconducting nature of the pseudogap in cuprates.

DIAGRAM COMBINATORICS FOR HEISENBERG PSEUDOGAP FLUCTUATIONS.

To analyze diagram combinatorics, let us consider the limit of infinite correlation length of pseudogap fluctuations. In this case the spin density scattering electrons takes the form:

$$\mathbf{S_q} = \mathbf{S}\delta(\mathbf{q}-\mathbf{Q}) \tag{37}$$

and averaging over Gaussian spin fluctuations reduces to the usual integration [4]:

$$< \ldots >= \frac{g^3}{(2\pi)^{\frac{3}{2}}W^3}\int d\mathbf{S}e^{-\frac{g^2\mathbf{S}^2}{2W^2}}\ldots \tag{38}$$

Accordingly, in this limit we can first solve the problem for an electron, moving in the coherent field of spin density (37), and afterwards perform averaging (38) over its fluctuations. For further analysis it is convenient to introduce fluctuating field $\delta = \frac{g}{\sqrt{3}}\mathbf{S}$ — "potential", scattering electrons. Then averaging (38) over spin fluctuations reduces to the averaging over fluctuations of this random field:

$$< \ldots >= \left(\frac{3}{2\pi W^2}\right)^{\frac{1}{2}}\int_{-\infty}^{+\infty} d\delta_l e^{-\frac{3\delta_l^2}{2W^2}}\frac{3}{2\pi W^2}\int_0^{2\pi}d\varphi\int_0^{+\infty}d|\delta_t||\delta_t|e^{-\frac{3|\delta_t|^2}{2W^2}}\ldots \tag{39}$$

We see that actually we have two fluctuating fields scattering electrons: the real longitudinal field $\delta_l = \frac{g}{\sqrt{3}}S_z$ and complex transverse δ_t, characterized by the amplitude $|\delta_t|$ and phase φ, connected with two transverse components of $\mathbf{S}$.

Such averaging generates diagram technique with two types of effective interactions [4]. One can be represented say by dashed interaction line and correspond to:

$$V_{eff1} = \frac{g^2}{3} < S_{z\mathbf{q}}S_{z-\mathbf{q}} >= \pm\frac{W^2}{3}\delta(\mathbf{q}-\mathbf{Q}) \tag{40}$$

where the sign "$-$" is taken when spin projection under this line is changed (e.g. when this dashed line surrounds an odd number of spin – flipping operators S_+, S_-), and another, represented by wavy line:

$$V_{eff2} = \frac{g^2}{3} < S_{+\mathbf{q}}S_{--\mathbf{q}} >= 2\frac{W^2}{3}\delta(\mathbf{q}-\mathbf{Q}) \tag{41}$$

The averages like $< S_+S_+ >$ and $< S_-S_- >$ are zero after averaging over the phase in (39).

Let us start with electron moving in coherent filed of spin density (37). In this case single – particle Green's function is represented by 2×2 matrix with 4 independent components[12], which are determined by the following system:

$$\begin{aligned}
G_{1\uparrow;1\uparrow} &= G_1 + G_1\delta_l G_{2\uparrow;1\uparrow} + G_1\delta_t G_{2\downarrow;1\uparrow}\\
G_{2\uparrow;1\uparrow} &= G_2\delta_l G_{1\uparrow;1\uparrow} + G_2\delta_t G_{1\downarrow;1\uparrow}\\
G_{2\downarrow;1\uparrow} &= -G_2\delta_l G_{1\downarrow;1\uparrow} + G_2\delta_t^* G_{1\uparrow;1\uparrow}\\
G_{1\downarrow;1\uparrow} &= -G_1\delta_l G_{2\downarrow;1\uparrow} + G_1\delta_t^* G_{2\uparrow;1\uparrow}
\end{aligned} \tag{42}$$

where we have introduced short notations: $(\varepsilon_n,\mathbf{p})\to 1$, $(\varepsilon_n,\mathbf{p}+\mathbf{Q})\to 2$ and $G_1 = \frac{1}{i\varepsilon_n - \xi_{\mathbf{p}}}$, $G_2 = \frac{1}{i\varepsilon_n - \xi_{\mathbf{p}+\mathbf{Q}}}$. Then we obtain:

$$\begin{aligned}
G_{1\uparrow;1\uparrow} &= \frac{G_2^{-1}}{G_1^{-1}G_2^{-1}-|\delta|^2}; \qquad & G_{2\uparrow;1\uparrow} &= \frac{\delta_l}{G_1^{-1}G_2^{-1}-|\delta|^2}\\
G_{1\downarrow;1\uparrow} &= 0; \qquad & G_{2\downarrow;1\uparrow} &= \frac{\delta_t^*}{G_1^{-1}G_2^{-1}-|\delta|^2}
\end{aligned} \tag{43}$$

where $|\delta| = \sqrt{\delta_l^2+|\delta_t|^2}$ is the amplitude of the field δ.

---

[12] Components differing from these by the change of all spin projections can be obtained by substitution: $\delta_l\to-\delta_l$, $\delta_t\leftrightarrow\delta_t^*$

The averaged Green's function is given now by:

$$G =< G_{1\uparrow;1\uparrow} >= \sqrt{\frac{2}{\pi}} \frac{1}{(W^2/3)^{\frac{3}{2}}} \int_0^{+\infty} d|\delta||\delta|^2 e^{-\frac{3|\delta|^2}{2W^2}} \frac{G_2^{-1}}{G_1^{-1}G_2^{-1} - |\delta|^2} \tag{44}$$

This integral form can be easily represented [4] by continuous fraction (1), (2) with $\kappa = 0$ with combinatorial coefficients $s(k)$, defined in (9).

Situation with combinatorial factors $r(k)$ for two – particle vertices is more complicated. In fact we have to consider four types of vertices, shown in Fig. 16. For all these vertices the recursion procedure has the form of (13), but signs and combinatorial factors $r(k)$ are different. Consider first all these vertices for an electron in coherent field δ.

1. Charged vertex (spin projection is conserved) in diffusion (particle – hole) channel (Fig. 16 (a)):

$$\Gamma_d^{ch} = \sum_{i,\sigma} G_{1\uparrow;i\sigma} G_{i'\sigma;1'\uparrow} = \frac{(G_2 G_{2'})^{-1} + |\delta|^2}{d_\delta} \tag{45}$$

where i and σ take the values 1, 2 and $\uparrow, \downarrow$, and we introduced notation $(\varepsilon'_n, \mathbf{p}') \to 1'$, $(\varepsilon'_n, \mathbf{p}' + \mathbf{Q}) \to 2'$ $d_\delta = [(G_1 G_2)^{-1} - |\delta|^2][(G_{1'} G_{2'})^{-1} - |\delta|^2]$

2. Charged vertex in Cooper (particle – particle) channel[13] (Fig. 16 (b)):

$$\Gamma_c^{ch} = \sum_{i,\sigma} G_{1\uparrow;i\sigma} G_{1'\uparrow;i'\sigma} = \frac{(G_2 G_{2'})^{-1} + \delta_l^2}{d_\delta} \tag{46}$$

3. Spin vertex (spin projection changes sign) in diffusion (particle – hole) channel (Fig. 16 (c)):

$$\Gamma_d^{sp} = \sum_{i,\sigma} G_{1\uparrow;i\sigma} G_{i'-\sigma;1'\downarrow} = \frac{(G_2 G_{2'})^{-1} - \delta_l^2}{d_\delta} \tag{47}$$

4. Spin vertex in Cooper (particle – particle) channel (Fig. 16 (d)):

$$\Gamma_c^{sp} = \sum_{i,\sigma} G_{1\uparrow;i\sigma} G_{1'\downarrow;i'-\sigma} = \frac{(G_2 G_{2'})^{-1} + (|\delta_t|^2 - \delta_l^2)}{d_\delta} \tag{48}$$

Physical vertices are obtained from these by averaging by fluctuations of coherent field δ with the help of (39).

Finally, we can see that the vertex Γ_d^{ch} is determined by Eq. (45), while all other vertices take the form[14]:

$$\Gamma = \frac{(G_2 G_{2'})^{-1} \pm \frac{1}{3}|\delta|^2}{d_\delta} \tag{49}$$

where "+" corresponds to vertices Γ_c^{ch} and Γ_c^{sp}, while "−" is taken for Γ_d^{sp}.

In case of the vertex Γ_d^{ch} we have, obviously, $r(k) = s(k)$. It follows directly from the fact that diagram expansion for the physical vertex $< \Gamma_d^{ch} >$ can be obtained by inserting of appropriate bare vertex into all electron lines in any arbitrary diagram for the single – particle Green's function. This insertion does not change the direction of either electronic line or spin projection, so diagram combinatorics does not change.

In the limit of infinite correlation length any "skeleton" diagram for the vertex differs from "ladder" diagram of the same order in interaction $\frac{W^2}{3}\delta(\mathbf{q} - \mathbf{Q})$ only by sign and the factor of 2^p, where p — is the number of wavy interaction lines. Thus, the sum of all "skeleton" diagrams in the given order reduces to the contribution of the appropriate "ladder" diagram with interaction $\frac{W^2}{3}\delta(\mathbf{q} - \mathbf{Q})$, multiplied by combinatorial factor, which we call the "number" of "skeleton" diagrams of the given order.

First term in Eqs. (45)-(48) is the same for all vertices and generates, after averaging procedure, the "numbers" of "skeleton" diagrams of even order in W^2 (this term corresponds to $i = 1$ contribution in these expressions). We see that the "numbers" of "skeleton" diagrams of even order are the same for all types of vertices. The second

---

[13] It appears in case triplet pairing.

[14] This form is equivalent to (46),(47),(48) after averaging

term in these expressions generates "numbers" of diagrams of odd order (corresponding to contributions with $i = 2$). Accordingly, the "numbers" of "skeleton" diagrams of odd order for three vertices, defined by (49), is equal to $\pm\frac{1}{3}$ of appropriate "numbers" for the vertex Γ_d^{ch}. The sign "$-$", corresponding to the vertex Γ_d^{sp}, may be compensated by appropriate change of sign in recursion procedure for this vertex. It follows that the sign before the second term in (49) determines the sign in recursion procedure (13) for these vertices, while combinatorial factors $r(k)$ for all three vertices are the same.

The "number" of "skeleton" diagrams of the order L is now[15]:

$$3^L \prod_{1 \le k \le L} r(k) \tag{50}$$

Thus, for even $L = 2n$ we obtain:

$$\prod_{1 \le k \le 2n} r(k) = \prod_{1 \le k \le 2n} s(k) \tag{51}$$

For odd $L = 2n + 1$:

$$\prod_{1 \le k \le 2n+1} r(k) = \frac{1}{3} \prod_{1 \le k \le 2n} s(k) \tag{52}$$

Then, taking into account (9), we immediately obtain (14).

In this paper we were mainly interested in the vertex Γ_c^{sp}. The analysis, performed above, shows that for this vertex we get the recursion procedure without alternating signs for the case of s-wave pairing, when symmetry factor $e(\mathbf{p})$ of the vertex is equal to 1. In case of d-wave pairing, when superconducting gap changes sign after change of the momentum by $\mathbf{Q}$ (i.e. $e(\mathbf{p}) = -e(\mathbf{p} + \mathbf{Q})$)), the sign in recursion procedure is changed to the opposite [6] and we obtain recursion procedure with alternating signs. Note, that in the case of Ising – like spin fluctuations, analyzed in Ref. [6], situation with signs in recursion procedure for the vertex is strictly opposite. This fact is easily understood from an expression (48) for the vertex Γ_c^{sp}. In Ising case two transverse components (i.e. the field δ_t) just disappear, leading to the sign change of the second term in (48) and in recursion procedure.

---

[15] The factor of 3^L appears due to the fact that both recursion procedure (13) and combinatorial coefficients $r(k)$ correspond to expansion in powers of W^2, while the "number" of "skeleton" diagrams is defined for an expansion in powers of $\frac{W^2}{3}$.

[1] J.L.Tallon, J.W.Loram. Physica C **349**, 53 (2000)
[2] M.V.Sadovskii. Physics Uspekhi **44**, 515 (2001)
[3] D.Pines. ArXiv: cond-mat/0404151
[4] J.Schmalian, D.Pines, B.Stojkovic. Phys.Rev. **B60**, 667 (1999)
[5] E.Z.Kuchinskii, M.V.Sadovskii. JETP **88**, 968 (1999)
[6] E.Z.Kuchinskii, M.V.Sadovskii, N.A.Strigina. JETP **98**, 748 (2004)
[7] N.A.Kuleeva, E.Z.Kuchinskii. Fiz. Tverd. Tela **46**, 1557 (2004)
[8] M.V.Sadovskii, N.A.Strigina. JETP **95**, 526 (2002)
[9] A.A.Abrikosov, L.P.Gorkov, I.E.Dzyaloshinskii. Methods of Quantum Field Theory in Statistical Physics. Pergamon Press, Oxford, 1965
[10] A.I.Posazhennikova, M.V.Sadovskii. JETP Lett. **63**, 358 (1996); JETP **85**, 1162 (1997)
[11] R.J.Radtke, K.Levin, H.-B.Schüttler, M.R.Norman. Phys.Rev. B **48**, 653 (1993)
[12] A.Posazhennikova, P.Coleman. Phys.Rev. **B67**, 165109 (2003)
[13] S.H.Naqib, J.R.Cooper, J.L.Tallon, R.S.Islam, R.A.Chakalov. ArXiv:cond-mat/0312443
[14] M.R.Presland, J.L.Tallon, R.G.Buckley, R.S.Liu, N.E.Flower. Physica C **176**, 95 (1991)
[15] A.E.Karkin, S.A.Davydov, B.N.Goshchitskii, S.V.Moshkin, M.Yu.Vlasov. Fiz. Metals – Metallogr. **76**, 103 (1993)
[16] Y.Fukuzumi, K.Mizuhashi, K.Takenaka, S.Uchida. Phys.Rev.Lett. **76**, 684 (1996)
[17] J.L.Tallon, C.Bernhard, G.V.M.Williams, J.W.Loram. Phys.Rev.Lett. **79**, 5294 (1997)
[18] S.K.Tolpygo, J.-Y.Lin, M.Gurvitch, S.Y.Hou, J.M.Phillips. Phys.Rev. B **53**, 12454, 12462 (1996)
[19] F.Rullier-Albenque, H.Alloul, R.Tourbot. Phys.Rev.Lett. **91**, 047001 (2003)
[20] M.V.Sadovskii. Superconductivity and Localization. World Scientific, Singapore 2000
[21] A.I.Posazhennikova, M.V.Sadovskii. JETP Lett. **65**, 270 (1997)
[22] G.Haran, A.D.S.Nagy. Phys.Rev. **54**, 15463 (1996)
[23] T.Valla, A.V.Fedorov, P.D.Johnson, Q.Li, G.D.Gu, N.Koshizuka. Phys.Rev.Lett. **85**, 828 (2000)
[24] A.Kaminski, H.M.Fretwell, M.R.Norman, M.Randeria, S.Rosenkranz, J.C.Campuzano, J.Mesot, T.Sato, T.Takahashi, T.Terashima, M.Takano, K.Kadowaki, Z.Z.Li, H.Raffy. Arxiv: cond-mat/0404385
[25] E.Z.Kuchinskii, M.V.Sadovskii. JETP **90**, 535 (2000)
[26] E.Z.Kuchinskii, M.V.Sadovskii. JETP **94**, 654 (2002)
[27] S.H.Pan, J.P.O'Neil, R.L.Badzey, C.Chamon, H.Ding, J.R.Engelbrecht, Z.Wang, H.Eisaki, S.Uchida, A.K.Gupta. Nature **413**, 282 (2001)
[28] K.McElroy, D.-H.Lee, J.E.Hoffman, K.M.Lang, E.W.Hudson, H.Eisaki, S.Uchida, J.Lee, J.C.Davis. ArXiv: cond-mat/0404005
[29] A.Fang, C.Howald, N.Kanenko, M.Greven, A.Kapitulnik. ArXiv: cond-mat/0404452

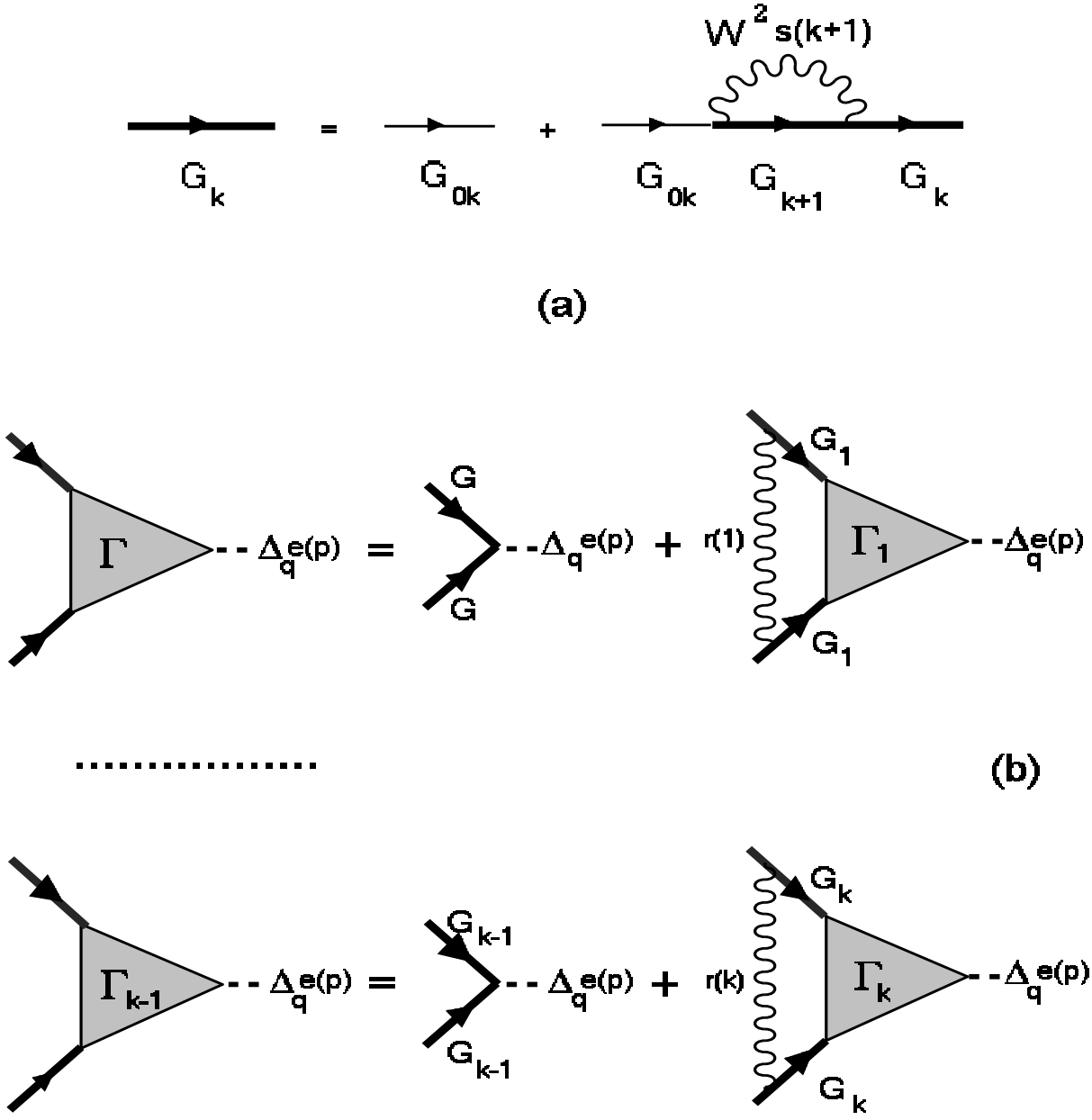

FIG. 1: Recurrence equations for Green's function (a) and "triangular" vertex (b).

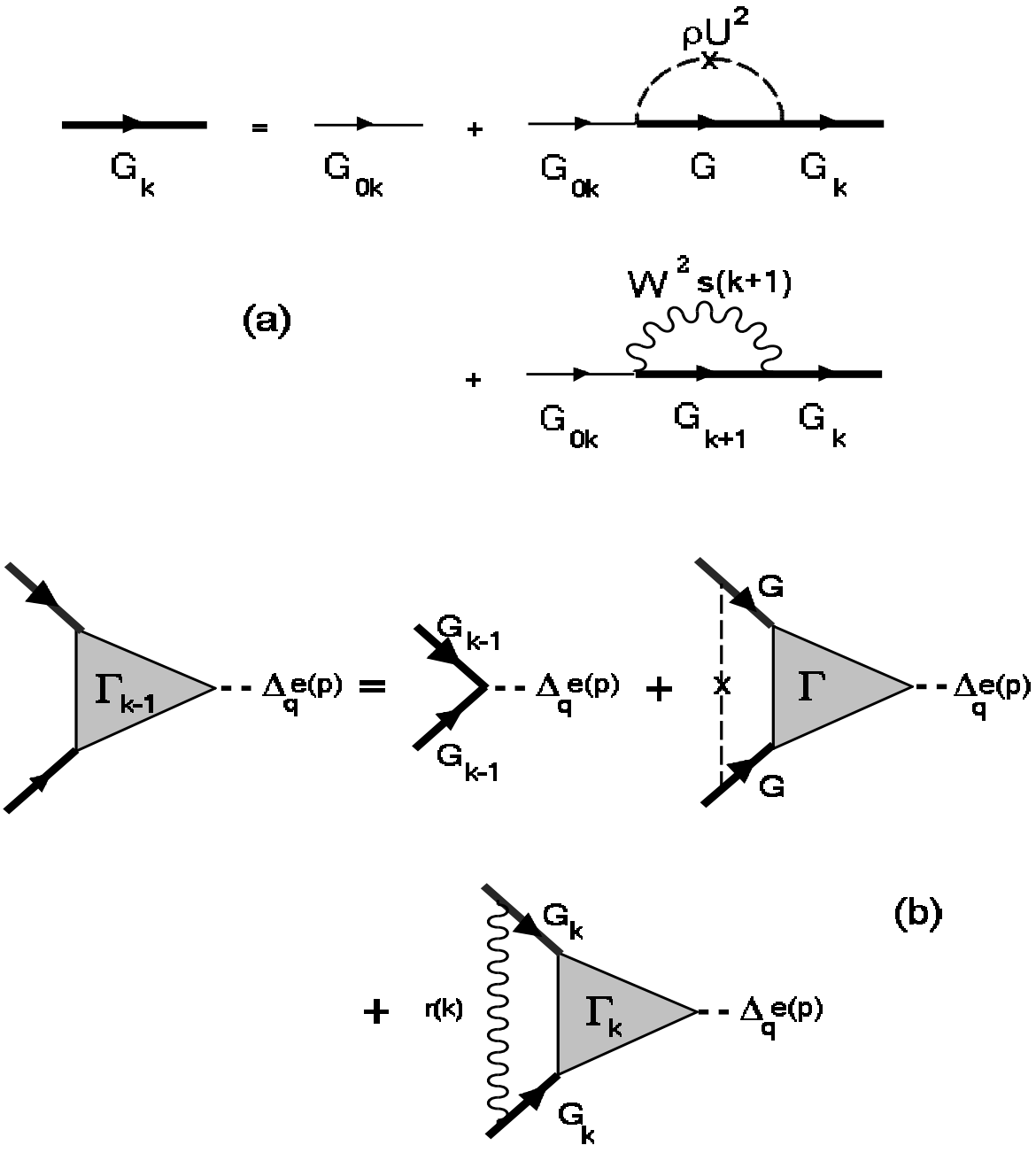

FIG. 2: Recurrence equations for Green's function (a) and "triangular" vertex (b) including scattering by random impurities.

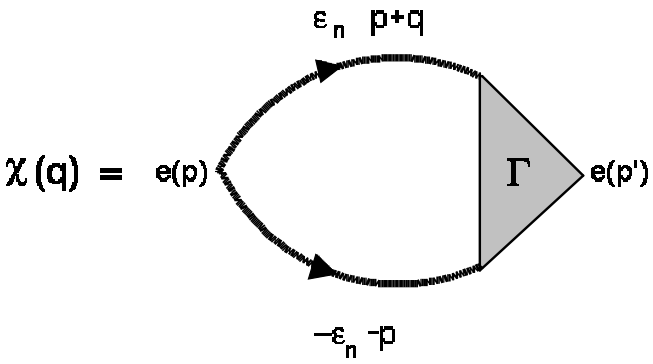

FIG. 3: Diagrammatic representation of the generalized Cooper channel susceptibility $\chi(\mathbf{q})$.

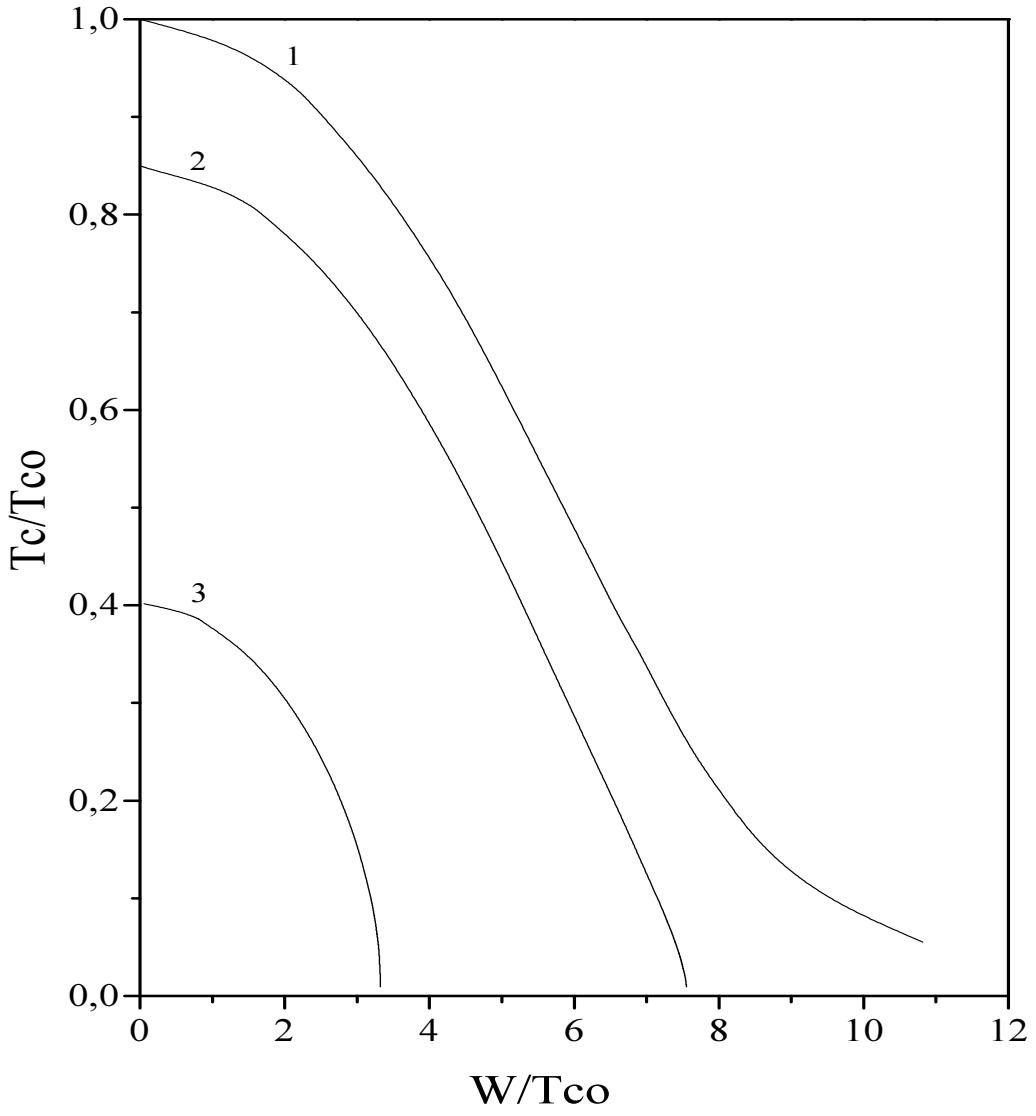

FIG. 4: T_c dependence on the effective width of the pseudogap W for the case of d-wave pairing and for several values of impurity scattering rate γ_0/T_{c0}: 0 – 1; 0.18 – 2; 0.64 – 3. Inverse correlation length of short – range order κa=0.2

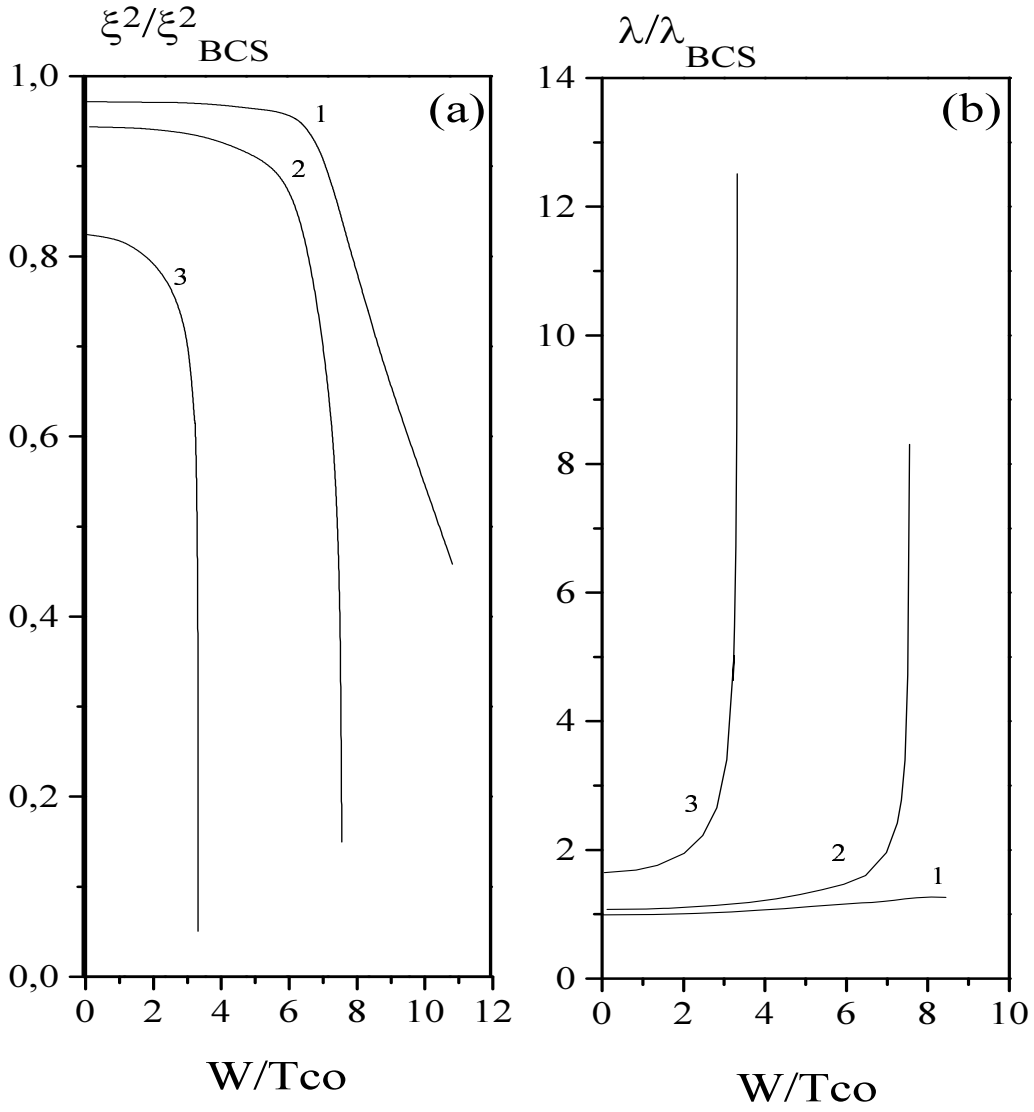

FIG. 5: Dependence of the square of coherence length and penetration depth on the effective width of the pseudogap W for the case of d-wave pairing and for several values of impurity scattering rate γ_0/T_{c0}: 0 – 1; 0.18 – 2; 0.64 – 3.

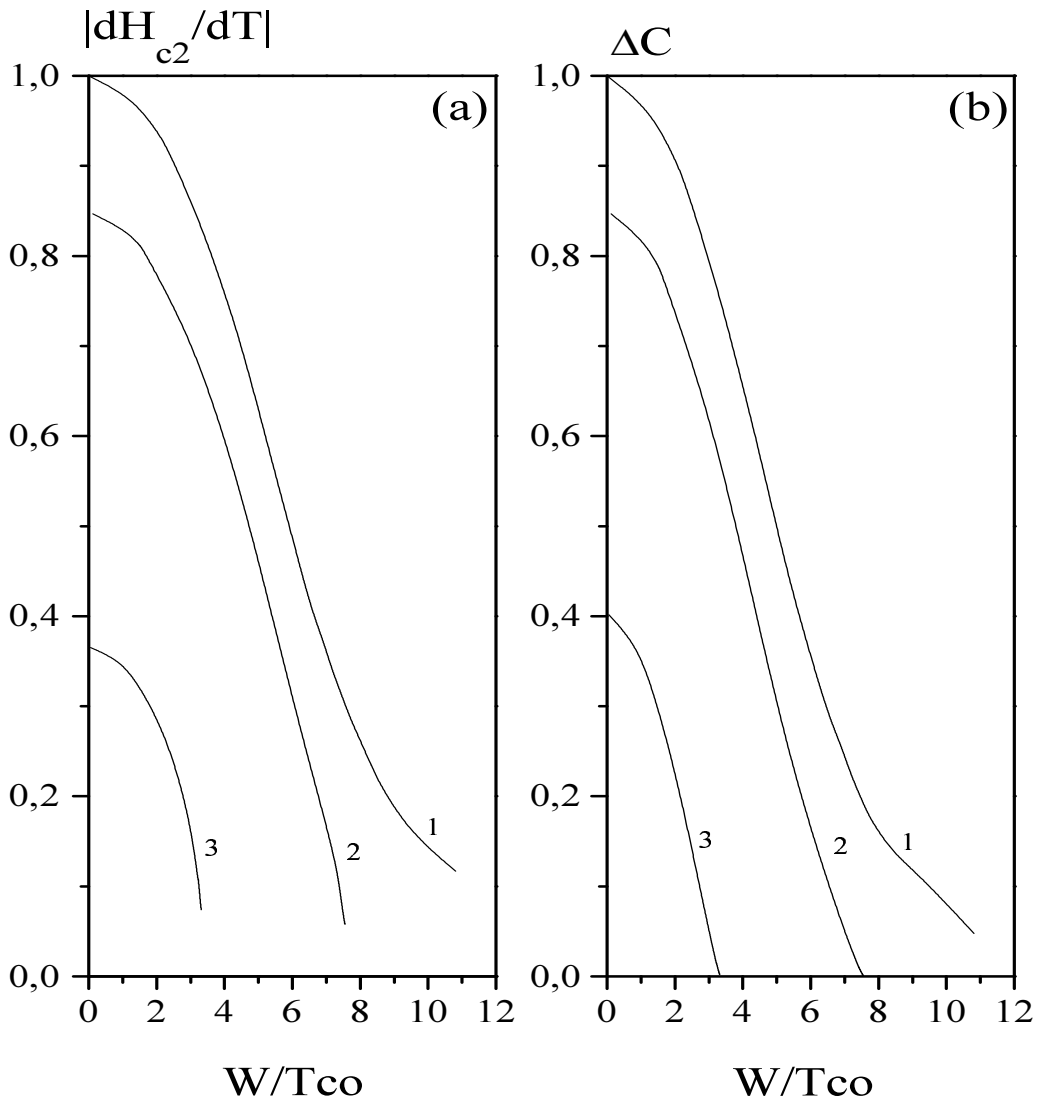

FIG. 6: Dependence of the slope of $H_{c2}(T)$ and specific heat discontinuity at superconducting transition on the effective width of the pseudogap W for the case of d-wave pairing and for several values of impurity scattering rate γ_0/T_{c0}: 0 – 1; 0.18 – 2; 0.64 – 3.

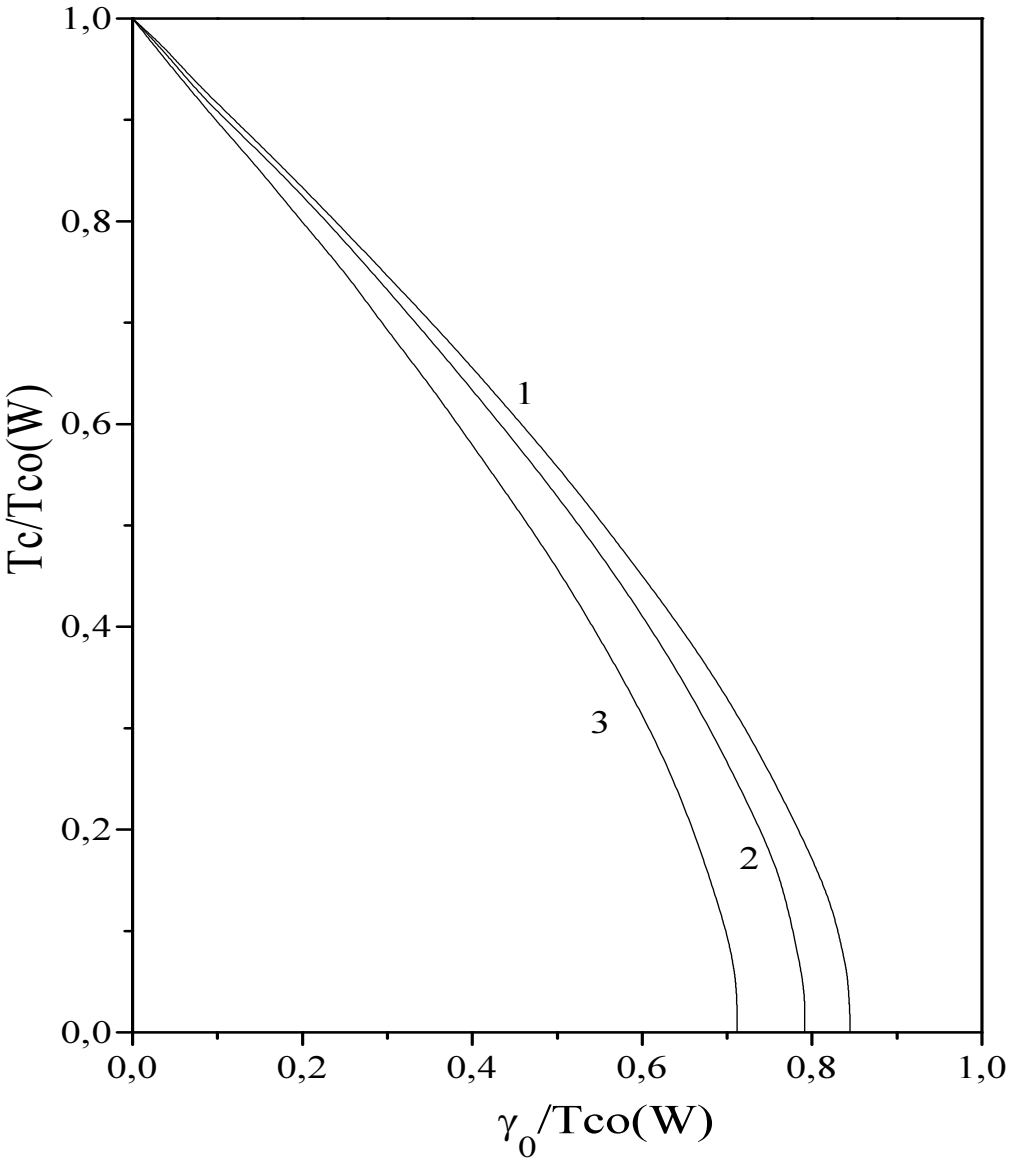

FIG. 7: T_c dependence on the impurity scattering rate (disorder) γ_0 for the case of d-wave pairing and for several values of the effective pseudogap width W/T_{c0}: 0 – 1; 2.8 – 2; 5.5 – 3.

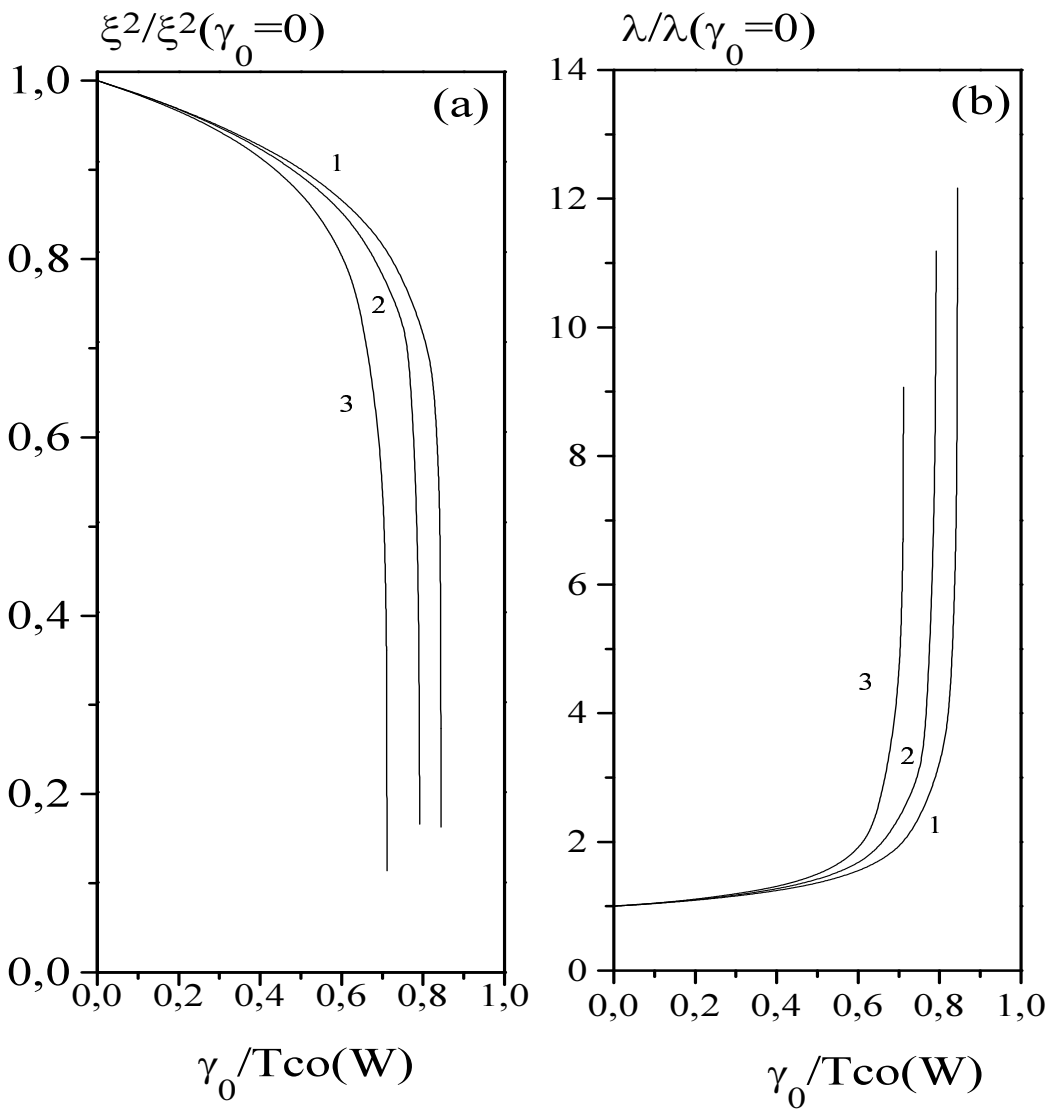

FIG. 8: Dependence of the square of the coherence length and penetration depth on the impurity scattering rate (disorder) γ_0 for the case of d-wave pairing and for several values of the effective pseudogap width W/T_{c0}: 0 – 1; 2.8 – 2; 5.5 – 3.

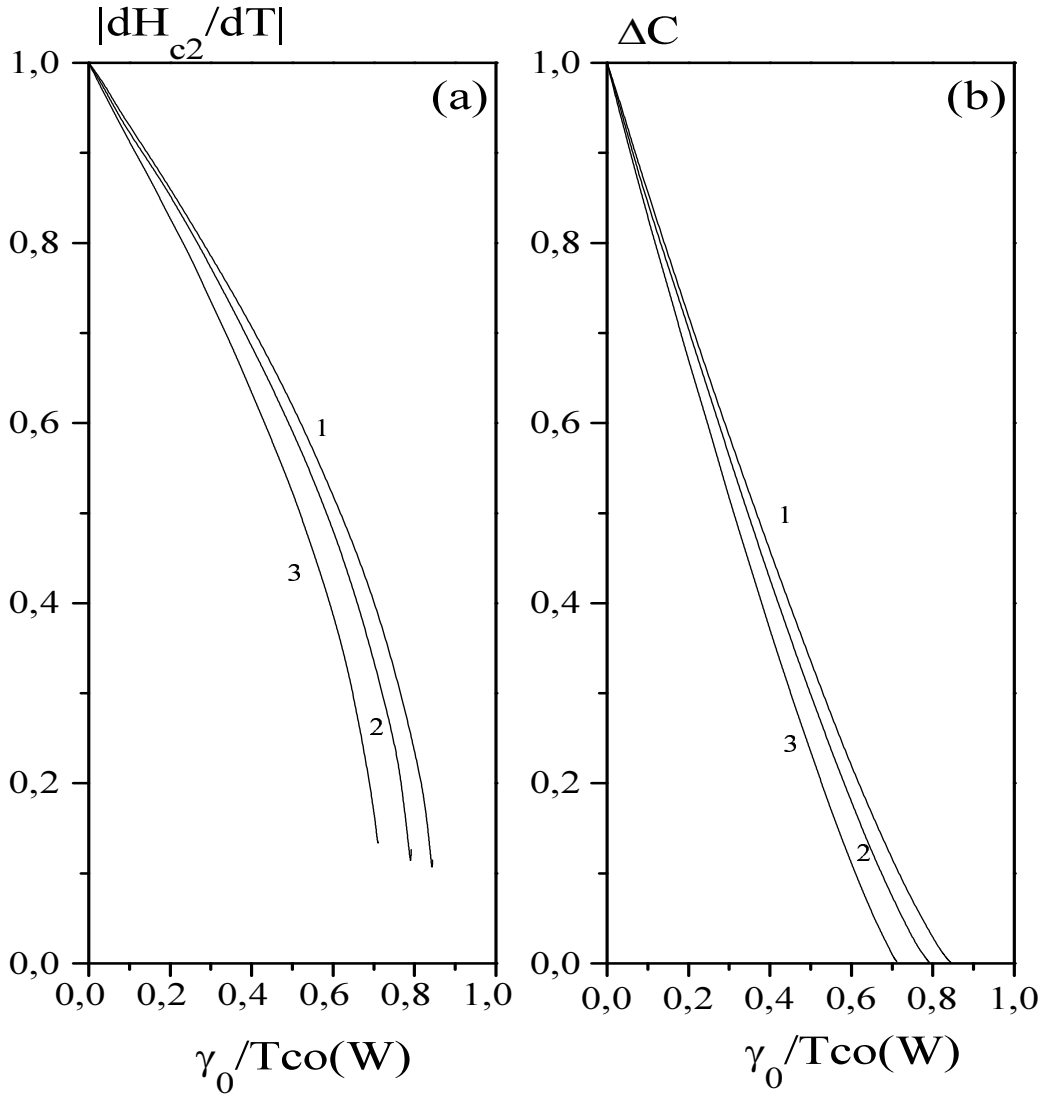

FIG. 9: Dependence of the slope of $H_{c2}(T)$ and specific heat discontinuity at superconducting transition on the impurity scattering rate (disorder) γ_0 for the case of d-wave pairing and for several values of the effective pseudogap width W/T_{c0}: 0 – 1; 2.8 – 2; 5.5 – 3.

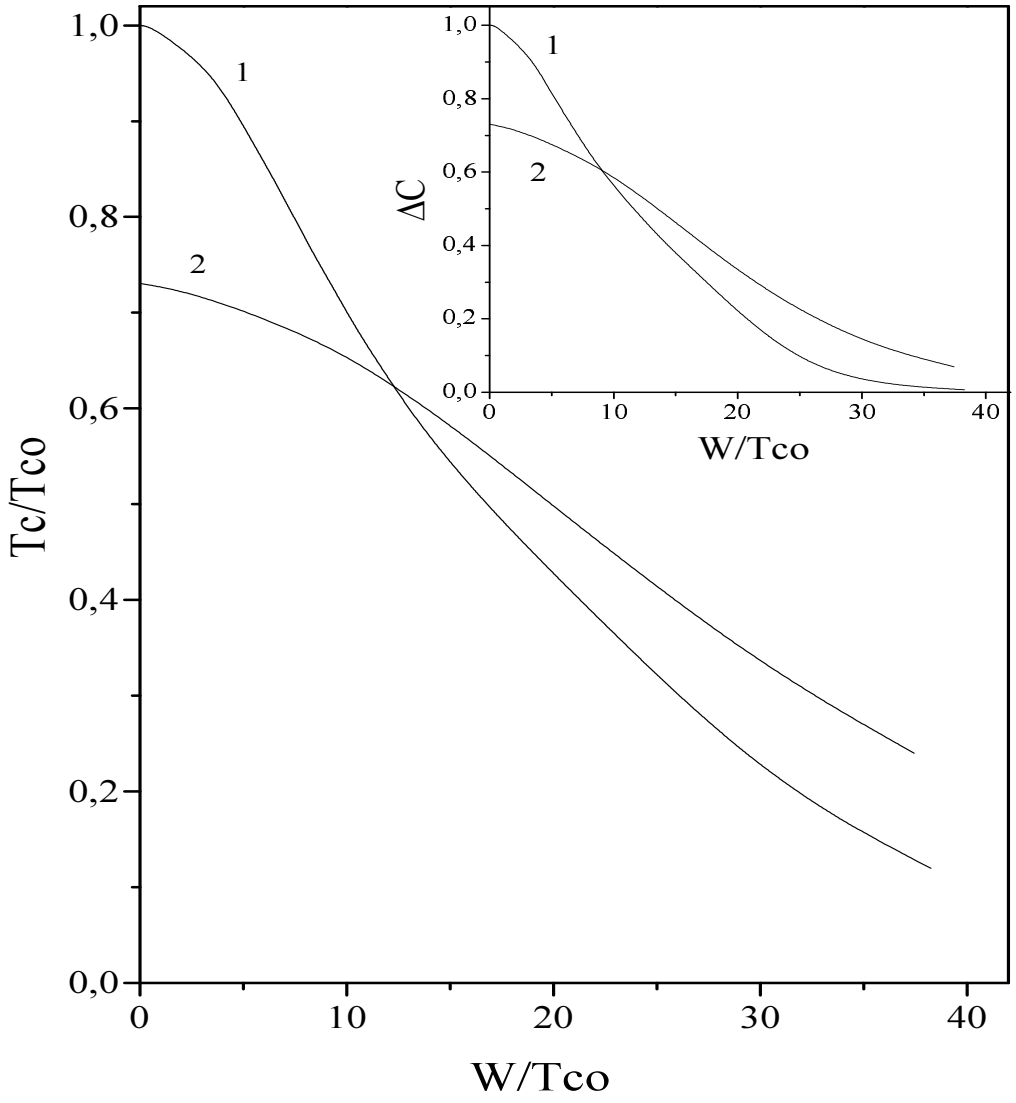

FIG. 10: T_c dependence on the effective width of the pseudogap W for the case of s-wave pairing and for two values of the impurity scattering rate γ_0/T_{c0}: 0 – 1; 20 – 2. Inverse correlation length of short – range order κa=0.2. At the insert — characteristic dependence of specific heat discontinuity for the same parameters.

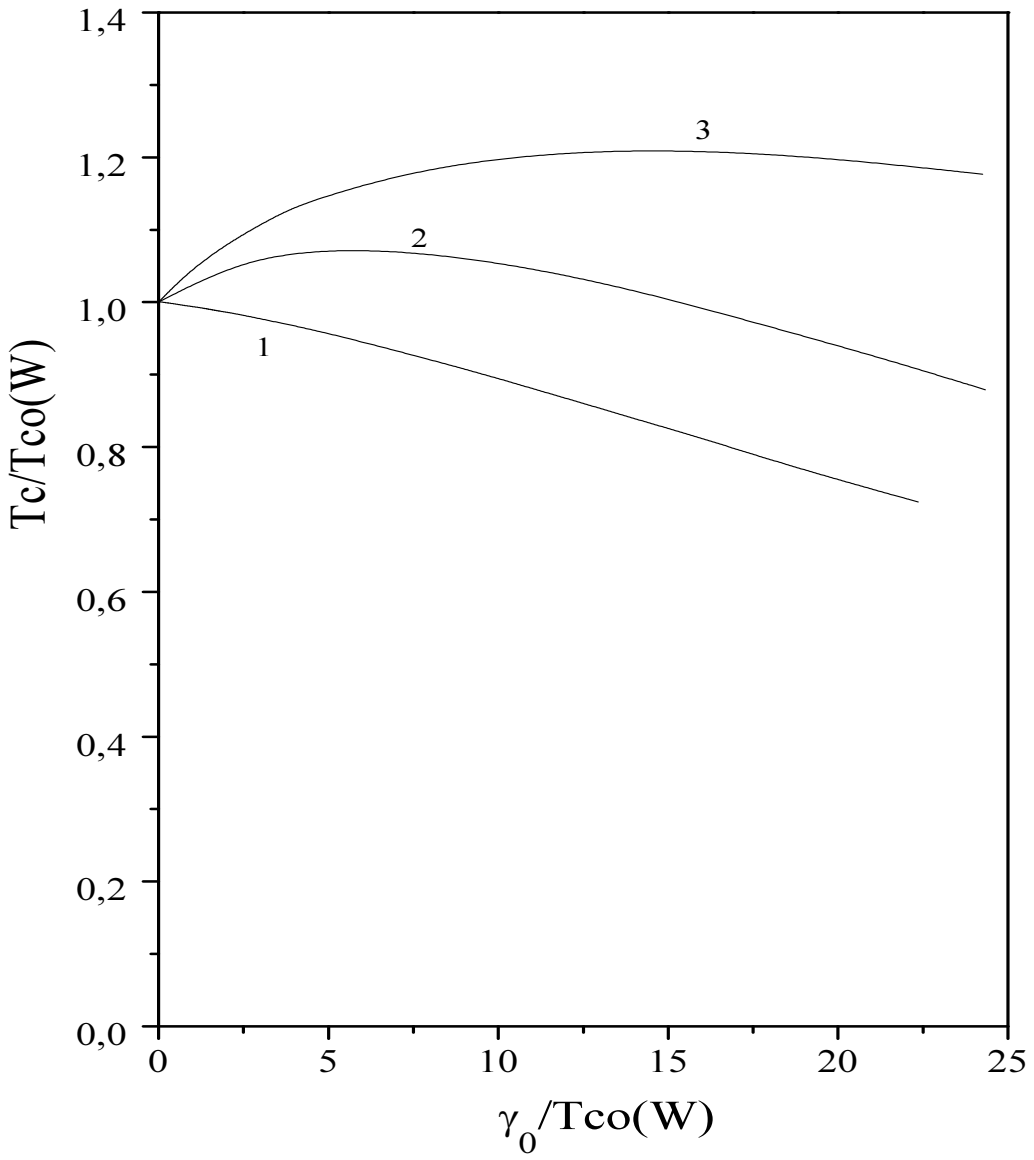

FIG. 11: T_c dependence on the impurity scattering rate (disorder) γ_0 for the case of s-wave pairing and for several values of effective pseudogap width W/T_{c0}: 0 – 1; 8 – 2; 15 – 3.

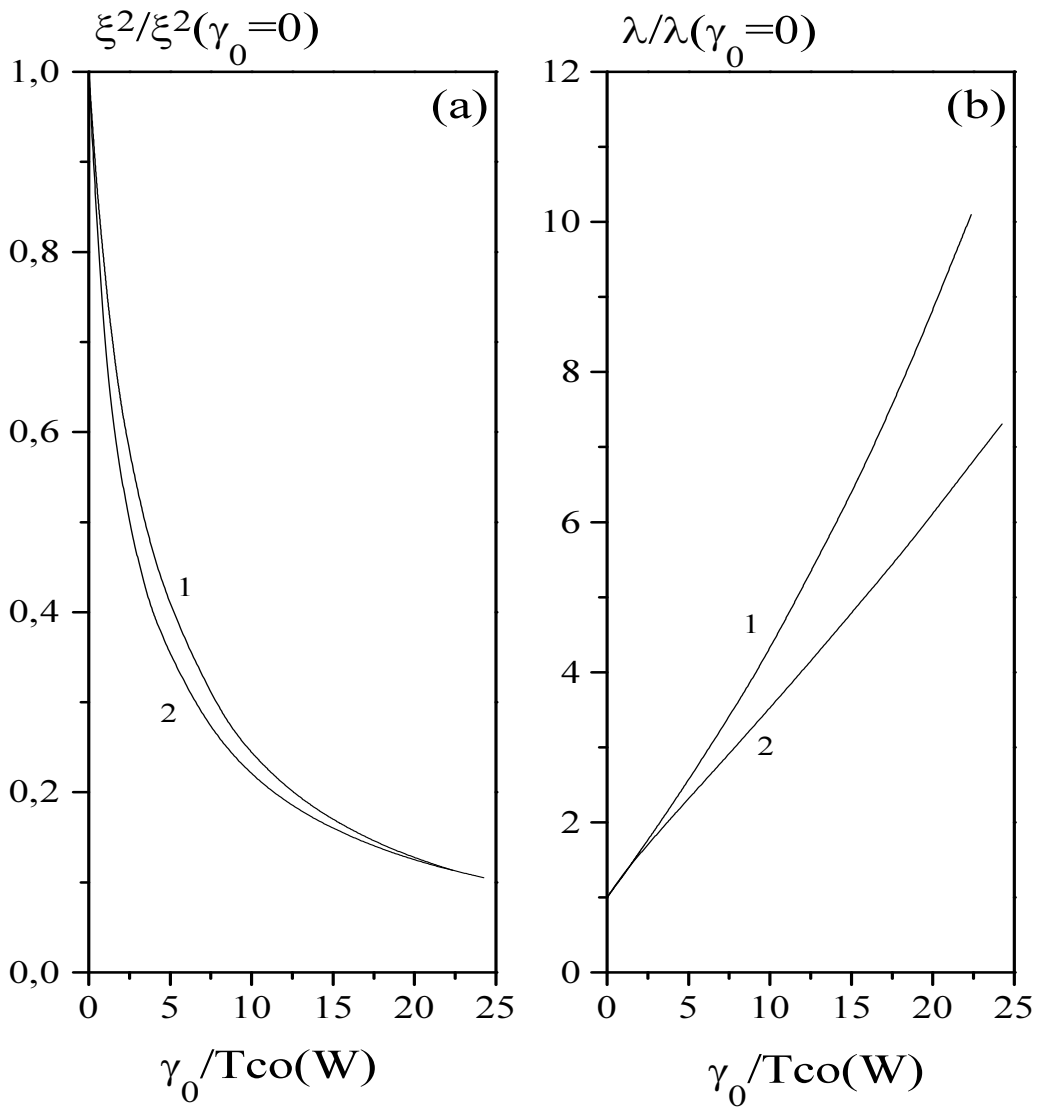

FIG. 12: Dependence of the square of coherence length and penetration depth on the impurity scattering rate (disorder) γ_0 for the case of s-wave pairing for two values of the effective pseudogap width W/T_{c0}: 0 – 1; 15 – 2.

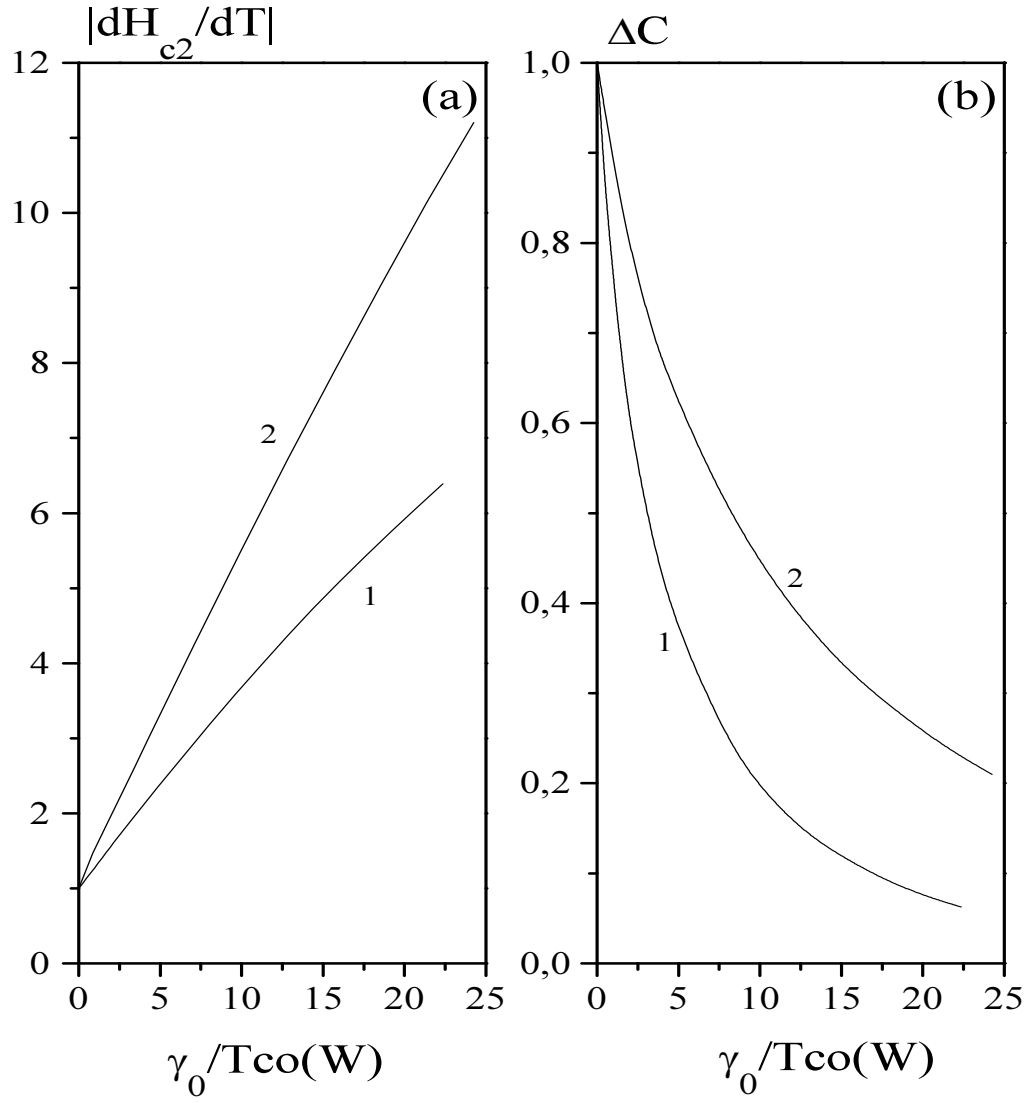

FIG. 13: Dependence of the slope of $H_{c2}(T)$ and specific heat discontinuity at the transition on the impurity scattering rate (disorder) γ_0 for the case of s-wave pairing and for two values of the effective pseudogap width W/T_{c0}: 0 – 1; 15 – 2.

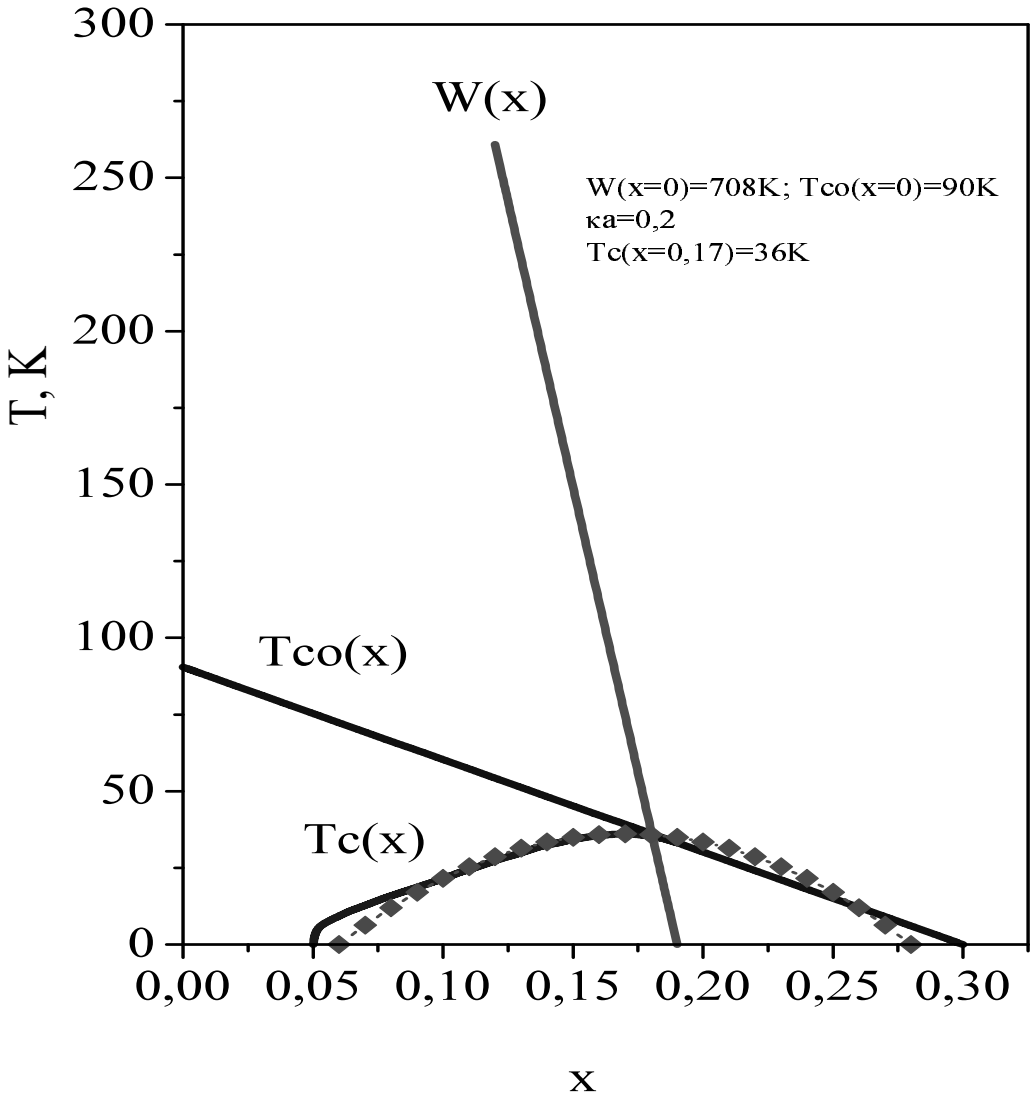

FIG. 14: Model phase diagram for the case of pseudogap fluctuations of CDW type (d-wave pairing) and "bare" superconducting transition temperature T_{c0} with linear dependence on carrier concentration.

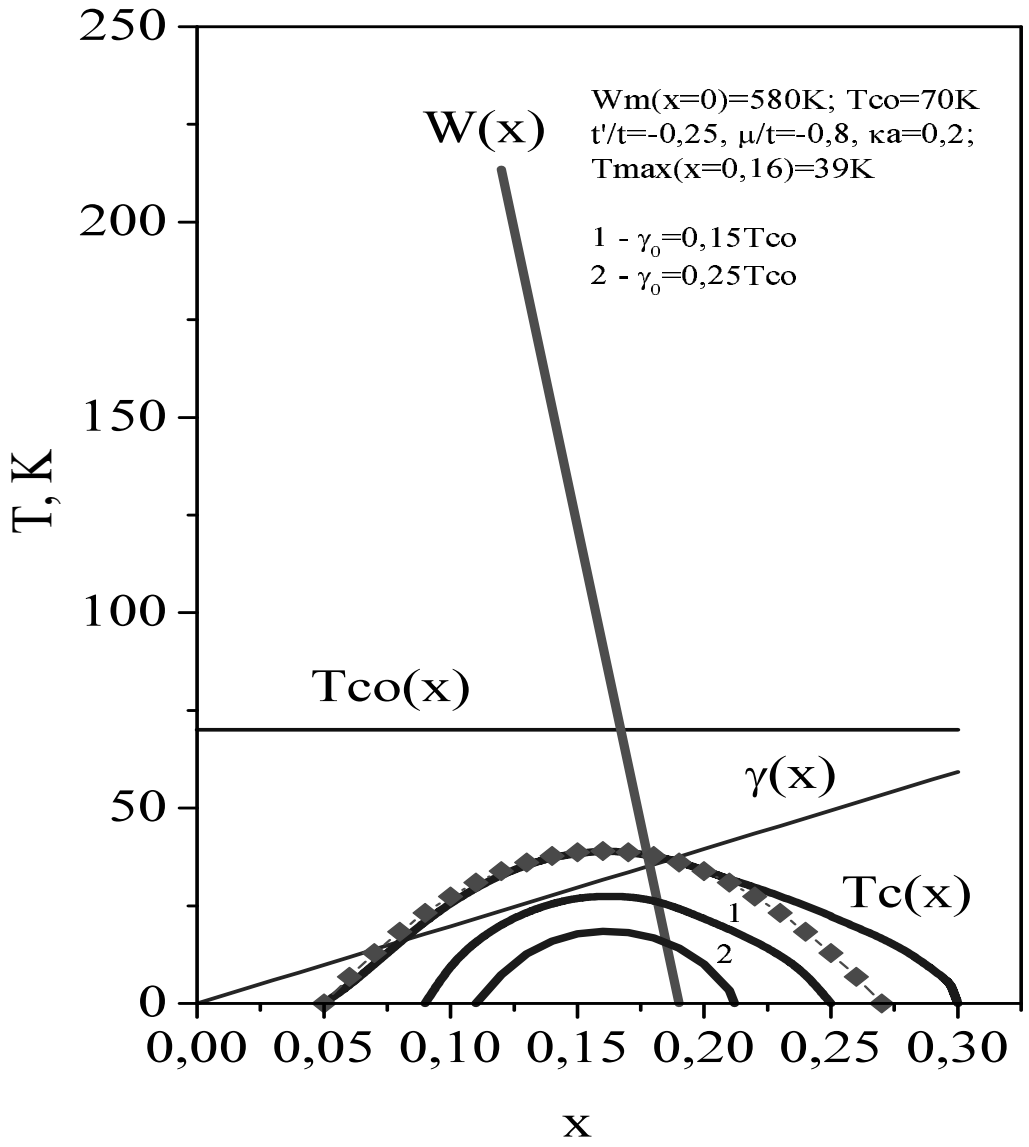

FIG. 15: Model phase diagram for the case of Heisenberg (SDW) pseudogap fluctuations (d-wave pairing) and "bare" superconducting transition temperature T_{c0} independent of carrier concentration, taking into account the role of internal disorder, linear over the concentration of doping impurity $\gamma(x)$.

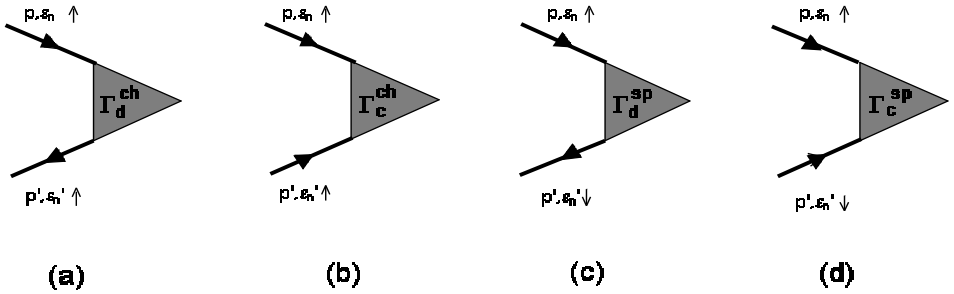

FIG. 16: Vertex parts with different diagram combinatorics.